~~Modification of methane oxidation pathways~~ ~~during long~~Long-term incubations ~~of methanic~~provide insight into the mechanisms of anaerobic oxidation of methane in methanogenic lake sediments

Hanni Vigderovich[a], Werner Eckert[b], Michal Elul[a], Maxim Rubin-Blum[c], Marcus Elvert[d], Orit Sivan[a]

[a] Department of Earth and Environmental Science, Ben-Gurion University of the Negev, Beer Sheva, Israel

[b] Israel Oceanographic & Limnological Research, The Yigal Allon Kinneret Limnological Laboratory, ~~Migdal,~~ Israel

[c] Israel ~~Limnology and Oceanography~~Oceanographic & Limnological Research, Haifa, Israel

[d] MARUM - Center for Marine Environmental Sciences and Faculty of Geosciences, University of Bremen, Bremen, Germany

Corresponding author: Hanni Vigderovich, hannil@post.bgu.ac.il

Abstract

Anaerobic oxidation of methane (AOM) is one of the major processes limiting the release of the greenhouse gas methane from natural environments. In Lake Kinneret ~~sediments, (~~Israel), geochemical profiles and experiments with fresh sediments indicate that iron-coupled AOM (Fe-AOM) ~~was suggested to play a substantial role (~~sequesters 10-15% ~~relative to methanogenesis)~~of the methane produced in the ~~methanic~~methanogenic zone (>20 cm sediment depth~~), based on geochemical profiles and experiments on fresh sediments. Apparently, the~~). The oxidation of methane ~~is~~in this environment was shown to be mediated by a combination of *mcr* gene ~~-~~bearing archaea and aerobic bacterial methanotrophs. Here, we aimed to investigate the ~~survival of this complex microbial interplay~~ AOM process in terms of various electron acceptors and involved microorganisms during long-term anaerobic sediment slurry incubations (~ 18 months) under controlled conditions. We followed the ~~AOM process during long-term (~ 18 months) anaerobic slurry experiments of these methanic sediments with~~ process with the addition of ^{13}C-labeled methane and two stages of incubations ~~and additions of ^{13}C-labeled methane, ~~: (i) enrichment of the microbial population involved in AOM and (ii) slurry dilution and manipulations, including addition of multiple electron acceptors (metal oxides, nitrate, nitrite and humic substances) and inhibitors~~. After these incubation stages carbon for methanogenesis/AOM and sulfate reduction. Carbon isotope measurements in the dissolved inorganic pool ~~still showed~~in these long-term incubations suggest that considerable AOM ~~(~~consumed 3-8% ~~relative to methanogenesis). Specific lipid carbon~~of the methane produced at a rate of 2.0±0.4 nmol gr^{-1} dry sediment day^{-1}. Carbon isotope measurements in lipids and metagenomic analyses indicate that ~~after the prolonged incubation aerobic methanotrophic bacteria were no longer involved in the oxidation process, whereas *mcr* gene bearing~~

Formatted: Header

Formatted: Space After: 8 pt

Formatted: Footer

~~archaea were most likely responsible for oxidizing the methane.~~only anaerobic microbes catalyzed this AOM. Whereas cryptic oxidation of methane by combining archaea and aerobic methanotrophs is feasible in the natural Lake Kinneret sediments, reverse methanogenesis dominates methane turnover in the long-term controlled experiments. Humic substances and iron oxides ~~are likely electron acceptors to support this oxidation, whereas~~ , but not sulfate, manganese, nitrate, and nitrite ~~did not support the AOM in these methanic sediments. Our results suggest in the natural~~ , are the likely electron acceptors used during the AOM. Our observations support the contrast between methane oxidation mechanisms in naturally anoxic lake sediments ~~methanotrophic bacteria are responsible for part of the methane oxidation by the reduction of combined micro-levels of oxygen and iron oxides in a cryptic cycle, while the rest of the methane is converted by reverse methanogenesis. After long-term incubation, the latter prevails without bacterial methanotropic activity and with a different iron reduction pathway.~~, with potentially co-existing aerobes and anaerobes, and long-term incubations, where anaerobes prevail.

Keywords

: Anaerobic oxidation of methane (AOM), ~~redox,~~ lake, sediments, dissolved inorganic carbon, stable ~~isotope~~isotopes, electron acceptor, methanotrophs

1. Introduction

Methane (CH_4) is an effective greenhouse gas (Wuebbles and Hayhoe, 2002) with anthropogenic and natural ~~origins~~sources. Natural methane ~~contributes~~sources contribute about 50% of ~~the global methane emissions~~this gas emission to the atmosphere (Saunois et al., 2020). Aerobic ~~as well as~~and anaerobic oxidation of methane (AOM) naturally control the release of this ~~greenhouse~~ gas to the atmosphere ~~from its natural sources~~ (Conrad, 2009; Reeburgh, 2007; Knittel and Boetius, 2009). While sulfate-dependent AOM, ~~which is~~ catalyzed by ANaerobic MEthanotrophs (ANMEs) 1-3, is widespread mostly in marine ~~environments~~sediments (Hoehler et al., 1994; Boetius et al., 2000; Orphan et al., 2001; Treude et al., 2005, 2014), in other environments methane oxidation ~~could theoretically~~can be coupled to other electron acceptors.

AOM coupled to the reduction of iron and manganese oxides has been ~~experimentally~~ confirmed in several ~~instances~~environments (Beal et al., 2009; Egger et al., 2015; ~~Sivan et al., 2011~~Sivan et al., 2011; Sivan et al., 2014; Segarra et al., 2013; Bar-or et al., 2017; Aromokeye et al., 2020; ~~Su et al., 2020). Humic substances, which shuttle electrons in anaerobic environments, may act as the terminal electron acceptors for AOM by ANME-2 (Scheller et al., 2016; Valenzuela et al., 2017; 2019; Bai et al., 2019).~~

~~There is also evidence that humic substances and synthetic analogs can stimulate metal-coupled AOM (Bond and Lovley, 2002; He et al., 2019; Valenzuela et al., 2019). Humic substances are considered complex organic compounds rich with redox functional moieties, such as quinones (Scott et al., 1998;~~

Formatted: Header

Formatted: Space Before: 12 pt, After: 0 pt

Formatted: Numbered + Level: 1 + Numbering Style: 1, 2, 3, … + Start at: 1 + Alignment: Left + Aligned at: 0 cm + Indent at: 0.63 cm

Field Code Changed

Formatted: Danish

Formatted: Danish

Field Code Changed

Formatted: Danish

Formatted: Danish

Formatted: English (United States)

Formatted: English (United States)

Field Code Changed

Formatted: Danish

Formatted: Danish

Formatted: Danish

Field Code Changed

Formatted: Danish

Formatted: Footer

~~Newman and Kolter, 2000; Ratasuk and Nanny, 2007), which provide these substances high redox capabilities (Valenzuela and Cervantes, 2021). The commercial quinone 9,10 anthraquinone 2,6-disulfonate (AQDS) can be used~~Su et al., 2020; Mostovaya et al., 2021). Alternative electron acceptors for AOM include other metals, humic substances, nitrate and nitrite. The synthetic analog for humic substances, 9,10-anthraquinone-2,6-disulfonate (AQDS), was shown to serve as a terminal electron acceptor (Scheller et al., 2016; Valenzuela et al., 2017; Bai et al., 2019; Zhang et al., 2019; Fan et al., 2020)~~ or an electron shuttle (Lovley et al., 1996; Newman and Kolter, 2000) for AOM. Nitrate dependent AOM have~~. Nitrate-dependent AOM has been demonstrated in a consortium of archaea and denitrifying bacteria (Raghoebarsing et al., 2006) and in an enrichment culture of ANME-2d (Haroon et al., 2013; Arshad et al., 2015), whereas nitrite fuels AOM by *Methylomirabilis* (NC-10, Ettwig et al., 2010). ANME-2d and *Methylomirabilis* can also couple AOM to selenite reduction (Luo et al., 2018). ~~It has also been shown that~~The ubiquitous aerobic methanotrophs Methylococcales~~, which usually require oxygen,~~ may ~~use~~oxidize methane ~~to support denitrification activity~~and denitrify under hypoxia (Kits et al., 2015), ~~and may couple methane oxidation and~~switch to iron reduction (Zheng et al., 2020)~~.~~ , or generate oxygen by methanobactins (Dershwitz et al., 2021). The latter study also showed the ability of alphaproteobacterial methanotroph *Methylocystis* sp. strain SB2 to couple methane oxidation and iron reduction.

In Lake Kinneret sediments, *in~~-~~situ* pore water profiles (~~Sivan et al., 2011)~~Sivan et al., 2011), diagenetic ~~modeling~~models (Adler et al., 2011) and incubation experiments with ~~freshly collected~~fresh sediment slurries (Bar-Or et al., 2017) ~~suggested~~suggest that iron reduction coupled to AOM (Fe-AOM) removes 10-15% of the produced methane in the deep ~~methanic~~methanogenic zone (>20 cm below water-sediment interface). Analysis of the microbial community structure revealed that both methanogenic archaea and methanotrophic bacteria are potentially involved in~~ the~~ methane oxidation (Bar-Or et al., 2015). Analyses of stable isotopes in fatty acids, the 16S rRNA gene amplicons and metagenomics ~~suggested~~showed that ~~archaea capable for~~ reverse methanogenesis ~~(probably *Methanothrix* or ANME-1)~~ by archaea and the bacterial type I aerobic ~~methanotrophs,~~methanotrophy by Methylococcales~~, and methylotrophs, *Methylotenera*,~~ play a role in methane cycling (Bar-Or et al., 2017; Elul et al., 2021). This aerobic methanotrophic activity has been observed in several anoxic hypolimnions and sediments of lakes (Beck et al., 2013; Oswald et al., 2016; Martinez-Cruz et al., 2017; ~~The metagenomics analysis together with the isotope enrichment of carbon in bacterial fatty acids following anoxic incubations of the fresh sediment slurries with ^{13}C-labelled methane (Bar-Or et al., 2017), provided evidence for the involvement of Methylococcales in methane oxidation~~Cabrol et al., 2020), and might be fueled by the presence of oxygen at microlevel up to several meters below the oxycline. However, whether these methanotrophs continue to oxidize methane under strictly anoxic conditions and which electron acceptors are available is still unknown.

Formatted: Header

Formatted: Danish

Formatted: Danish

Field Code Changed

Formatted: Font: Not Italic

Formatted: Footer

~~This activity of aerobic methanotrophs has been observed in several anoxic lakes' hypolimnions and sediments~~Here, we used long-term anaerobic incubations to assess the dynamics of methane-oxidizing microbes under anoxic conditions and to quantify various electron acceptors' availability for AOM. For this purpose, we diluted fresh methanogenic sediments from Lake Kinneret with original porewater from the same depth and amended the sediment with ^{13}C-labeled methane, following its oxidation to dissolved inorganic carbon (DIC). Our experiment design consisted of two stages, the first stage included the enrichment of the microbial population involved in AOM, and the second stage involved an additional slurry dilution and several manipulations with multiple electron acceptors and inhibitors. The potential electron acceptors were iron and manganese oxides, nitrate, nitrite and humic substances. We inhibited the *mcr* gene with 2-bromoethanesulfonate (BES), methanogens with acetylene and sulfate reduction and sulfur disproportionation with Na-Molybdate (Nollet et al., 1997; Orembland & Capone, 1988; Lovley & Klug, 1983). We measured methane oxidation rates (by the ^{13}C-DIC enrichment), the electron acceptor characteristics (by their addition or inhibition) and the evaluated changes in microbial diversity over various incubation periods (based on metagenomics and lipid biomarkers). The results from the long-term anaerobic incubations were compared to those of batch and semi-bioreactor experiments that were set up with fresh sediments to follow the changes in methane oxidation mechanisms.

~~(Beck et al., 2013; Oswald et al., 2016; Martinez-Cruz et al., 2017; Cabrol et al., 2020), and has been speculated by potential presence of micro levels of oxygen in the deep hypolimnion or sediments, even several meters below the oxycline. Methane oxidation by pure cultures of several different aerobic methanotrophs under hypoxia was attributed to an ability to survive by switching to iron reduction (Zheng et al., 2020) or by self-generation of oxygen by methanobactins (Dershwitz et al., 2021). The latter study also showed the ability of *Methylocystis* sp. Strain SB2, a specific alphaproteobacterial methanotroph, to reduce iron by methane in these unique conditions.~~

~~Here, we explored the role of methanotrophic activity in natural methanic lake sediments, its survival outside of the natural conditions during long-term anaerobic incubations, and whether there is a shift in the potential electron acceptors. To answer these questions, we diluted fresh methanic sediments from Lake Kinneret with porewater from the same depth twice and amended the sediment with ^{13}C-labeled methane to follow its oxidation to dissolved inorganic carbon (DIC). These incubations were then also amended with several types of potential electron acceptors and different inhibitors. The results of these experiments were compared to batch and semi-bioreactor experiments that were set up with freshly collected sediments to follow the changes in methane oxidation pathways along the incubation period. We also calculated methane oxidation and production rates of representative pre-incubated long-term slurry experiments. Alongside the ^{13}C-labeled DIC measurements, we investigated the structure of the microbial population using metagenomics and lipid biomarkers to identify the potential microbial players and their dynamics over various incubation periods.~~

Formatted: Header

Formatted: Footer

2. Methods

2.1 Study site

Lake Kinneret (Sea of Galilee) is a warm monomictic freshwater lake~~,~~ located in the North of Israel. The lake is 21 km long and 13 km wide. Its maximum depth is ~42 m at the lake center (station A, Figure S1) and the average depth is 24 m. The lake is thermally stratified from March ~~until~~to December, with the hypolimnion turning anoxic ~~starting~~ from April. ~~The sediment is~~Surface water temperatures range from 15 to 30 °C, and the bottom water temperatures remain between 14-17 °C all year long. The lake sediments are composed mostly of carbonates (40-50%) and clays (20%; ~~Hadas and Pinkas, 1995)~~Hadas and Pinkas, 1995; Eckert, 2000). The total iron content in the top 40 cm of the sediments is ~3 wt % (Serruya, 1971; Eckert, 2000; Bar-Or et al., 2017). The ~~composition of the~~ sediment at the deep ~~methanic depth~~methanogenic zone used in this study (~20 cm sediment depth~~) was similar with~~ from the water-sediment interface at the lake's center) contains 50% carbonates, 30% clay and 7% iron (Table S1). The porewater's dissolved organic carbon (DOC) concentration ~~in the porewater~~ increases with depth, ranging from ~6 mg C L^{-1} at the sediment-water interface to 17 mg C L^{-1} at 25 cm depth (Adler et al., 2011). Dissolved methane concentrations in the porewater increase sharply from the top sediments to more than 2 mM at 15 cm depth and then decrease to 0.5 mM (Adler et al., 2011; Sivan et al., 2011; Bar-Or et al., 2015).

2.2 Experimental set-up

This study compares three incubation strategies ~~with~~ (A, B and C) of Lake Kinneret methanogenic sediments amended with original porewater from the same depth, ^{13}C-labeled methane, different potential electron acceptors for AOM (~~NO_2^-, NO_3^-,~~nitrite, nitrate, metal oxides and humic substances) and inhibitors for sulfur cycling and ~~methanogens'~~methanogens' activity (~~details below) (~~Fig. 1):

~~1) Two-~~A) Long-term two-stage slurry incubations with a first stage of 1:1 sediment ~~- pore water~~to porewater ratio for three months~~, followed by a 1:~~ with high methane content to enrich the microorganisms involved in the AOM. After three months, the slurry was diluted to a 1:3 ratio ~~and the addition of~~ , then different ~~manipulations~~reactants were added to the incubations, which were monitored for up to 18 months.

~~2~~B) Semi-continuous bioreactor experiments with freshly collected ~~methanic~~ sediments and porewater ~~with~~at a 1:4 ratio~~.~~ (respectively), where porewater was exchanged regularly.

~~3) Our previous results gained from batch~~C) Batch incubation experiments with ~~freshly collected methanic~~fresh sampled sediments and porewater ~~with~~at a 1:~~3~~5 ratio, respectively, and several manipulations (this experimental set-up was described in our previous studies (Bar-Or et al., 2017; Elul et al., 2021~~).~~)).

Formatted: Header

Formatted: No underline

Formatted: Indent: Before: 0 cm

Formatted: Footer

Here below we describe the experiments. Detailed protocols are found in the supplementary information.

2.2.1 ~~Two-~~Experiment set-up A: Long-term two-~~-~~stage incubations

The sediments for the slurries were collected during several sampling campaigns between 2017 and 2019 from the central lake (Station A~~) and pooled~~, Fig. S1) using a gravity corer with 50 cm Perspex cores. Sediments from the ~~methanic~~methanogenic zone ~~(25 - 40 cm).~~(> 20 cm depth) were diluted with porewater from the methanogenic zone of parallel cores sampled on the same day. The ~~sediment was diluted under continuous flushing of N_2 gas with~~ porewater was extracted by centrifugation ~~from the same zone~~ at 9300 g for 15 minutes, filtered by 0.22 µM filters into 250 ml glass bottles, sealed with a rubber stopper, and flushed for 30 minutes with N_2.

In the first stage, the sediment was diluted with the extracted porewater to create a 1:1 ~~sediment - pore water~~ ratio slurry ~~(Fig. 1)~~ in 250 ml glass bottles with a headspace of 70-90 ml~~.~~ under continuous N_2 flushing (Fig. 1). The slurries were flushed with N_2 (99.999 %, MAXIMA, Israel) for 30 minutes~~, after which methane gas~~. Methane was injected ~~to reach 20 % of each bottle~~using a gas-tight syringe for a final content of 20% in the headspace, where 10 % of the injected methane was ^{13}C-labeled methane (99 %, Sigma-Aldrich~~) using a gas-tight syringe. After three months of~~). When significant AOM was observed by the increase of $\delta^{13}C_{DIC}$ after three months (Fig. S2), the incubations were either transferred to the second stage experiments or continued to run with porewater exchange and $\delta^{13}C_{DIC}$ values monitored every three months.

This study presents ten sets of two-stage incubation experiments with different treatments (electron acceptors/shuttling/inhibitors). They were all set up similarly (protocols in the supplementary information): subsamples (~18 g each) of the pre-incubation~~, when ^{13}C-labeled DIC was observed (Fig S1), subsamples (18 g each)~~ slurry were transferred with a syringe under continuous flushing of N_2 gas into 60 ml glass bottles and diluted with fresh ~~anaerobic~~anoxic porewater from the methanogenic zone (as described above) to achieve a 1:3 sediment ~~- pore water~~to porewater ratio (Fig. 1), ~~which leaves~~leaving 24 ml of headspace in each experiment bottle. ~~All pre-incubated experiment~~The bottles were crimp-sealed, flushed with N_2 gas for 5 minutes, shaken vigorously and flushed again (3 times). ^{13}C-labeled methane was added to all the bottles as described in Table 1. The "killed" control bottles in each experiment were autoclaved twice, cooled, and only then were amended with the appropriate treatments and ^{13}C-labeled methane.

~~To verify the role of different potential electron acceptor/s and inhibitors we conducted ten experiments as outlined in Table S2. The possible influence of sulfate reduction and sulfur disproportionation on AOM was investigated by adding~~Electron acceptors were added either as a powder (hematite, magnetite, clay, MnO_2, humic substances) or in dissolved form in double-distilled water (DDW) (KNO_3 and $NaNO_2$). The involvement of sulfur cycling was tested by inhibition with Na-molybdate (Lovley

Formatted: Header

Formatted: No underline

Formatted: Line spacing: Multiple 1.08 li

Formatted: Space Before: 0 pt, After: 8 pt

Formatted: Footer

and Klug, 1983), ~~to an already running experiment in case of an active cryptic sulfur cycle, even with the absence of detectable sulfate (Holmkvist et al., 2011). Other inhibitors added were 2-bromoethanesulfonate (BES, Nollet et al., 1997) and acetylene (Oremland and Capone, 1988) (Table S2). BES is a specific inhibitor for methanogens and ANME's *mcrA* genes, and acetylene is a non-specific inhibitor for methanogens (among others, as discussed later). BES was added at the beginning of the experiment, while acetylene gas was injected during the experiment to two bottles at different timepoints. Electron acceptors were added either as powder (hematite, magnetite, clay, MnO_2, humic substances) or in dissolved form (KNO_3 and $NaNO_2$). AQDS and phenazine-1-carboxylate (PCA) were dissolved in double distilled water (DDW) and then added. Amorphic iron ($Fe(OH)_3$) was prepared in the lab, by dissolving $FeCl_3$ in DDW, which was then titrated with NaOH 1.5 N, until the solution reached pH 7. The $Fe(OH)_3$ was added to the bottles by injection. The final concentration of each addition is described in table S2. The ^{13}C-labeled methane was injected into all experiment bottles~~while the other electron acceptors were tested for their potential participation by their addition to the slurries. AQDS was added as an analog for humic substances, which was previously shown to serve as a terminal electron acceptor for AOM and electron shuttling for iron reduction (e.g., Scheller et al., 2016; Sivan et al., 2016). Amorphous iron ($Fe(OH)_3$) was prepared in the lab by dissolving $FeCl_3$ in DDW, then titrated with NaOH 1.5 N up to pH 7 and was added to the bottles by injection. The final concentration of each addition is detailed in Table 1. The ^{13}C-labeled methane was injected to all experiment bottles at the beginning of each experiment (unless mentioned otherwise) using a gas-tight syringe from a stock bottle filled with ^{13}C-labeled methane gas (which was replaced with saturated NaCl solution). ~~Electron acceptors and ^{13}C-labeled methane were added to the "killed" control bottles after they were autoclaved twice and cooled. The variations in the $\delta^{13}C_{DIC}$ values between the experiments are the result of different amounts of ^{13}C-labeled methane injected at the start of each experiment. 2 ml of porewater were sampled anaerobically for $\delta^{13}C_{DIC}$ (duplicates were taken from each experimental bottle) and dissolved Fe(II) concentrations during each sampling point from all experimental bottles. Methane was measured from the headspace (duplicates from each experimental bottle) and the porewater concentrations were calculated using the volume of the bottles and the slurries. All live treatments were set up in duplicates or triplicates, except for the black coffee treatment, which only had one replicate as an attempt to check a close analog for humic substances. In 4 experiments only one "killed" control bottle was set up because these controls had been showing repetitive results (no activity) for numerous previous experiments. For the humic substrate experiment we received natural humic substance extracted from a lake by a colleague in the University of Alaska, Fairbanks. One experiment was set up without any additional electron acceptor in order to assess the rate of methanogenesis in the pre-incubated slurries.~~Three different inhibitors were added to three different experiments: molybdate, BES and acetylene. Molybdate was added to experiment No. 1 to detect the feasibility of an active sulfur cycle. BES was added to experiment No. 8 at the start of the experiment. Acetylene was added to experiment

Formatted: Header

Formatted: Footer

No. 9. It was injected during the experiment to two bottles at different timepoints after ^{13}C enrichment in the DIC was observed (Table 1).

~~2.2.2 Semi-bioreactor experiment~~

All live treatments were set up in duplicates or triplicates and we present the average with an error bar. In two experiments, only one "killed" control bottle was set up. The slurry was prioritized for other treatments since the killed controls showed repetitive no activity for numerous previous experiments. The humic substrate experiment used natural (humic) substance that were extracted from a different lake. One experiment was set up without any additional electron acceptor to assess the rate of methanogenesis in the two-stage slurries. Porewater was sampled anaerobically for $\delta^{13}C_{DIC}$ and dissolved Fe(II) measurements in duplicates (2 ml), and methane was measured from the headspace. Variations in the $\delta^{13}C_{DIC}$ values between the experiments resulted from different amounts of ^{13}C-labeled methane injected at the start of each experiment.

2.2.2 Experiment set-up B: Semi-bioreactor

Semi-bioreactors regularly monitored the redox state at close-to-natural *in-situ* conditions for 15 months in freshly collected sediments. Two 0.5 L semi-bioreactors (Fig. ~~1~~1) (LENZ, Weinheim, Germany) were set up with fresh sediments from the ~~methanic~~methanogenic zone (25 - 40 cm) of Lake Kinneret ~~central station (~~Station A~~)~~ immediately after their collection. Both reactors were filled headspace-free with a slurry ~~of~~at a 1:4 sediment - pore water ratio. One of the bioreactors was amended with 10 mM hematite~~.~~ and the second without it, serving as a control. To dissolve ^{13}C-labeled methane in the porewater, 15 ml of ~~headspace was produced~~porewater were replaced with ~~only~~15 ml of methane gas (a mixture of $^{12}CH_4$ and $^{13}CH_4$) to produce methane-only headspace for 24 hours. The reactors were shaken repeatedly during those hours. After 24 hours, the gas was replaced with anoxic ~~pore-water~~porewater, so that there was no ~~head-space~~headspace at all. ~~The oxidation-reduction~~This resulted in lower methane concentrations than the batch experiments (0.2 mM vs. ~2 mM, respectively). Redox potential was monitored continuously by ~~a redox~~ electrode (Metrohm, Herisau, Switzerland) ~~throughout the incubation period~~ to verify anoxic conditions and ~~to know~~determine the redox state ~~of~~throughout the ~~slurry in the reactor~~incubation period. The bioreactors were subsampled weekly to bi-weekly, and the sample volume (5-10 ml) was replaced immediately by preconditioned anoxic (flushed with N_2 gas for 15 minutes ~~before the exchange~~) porewater from the ~~methanic~~methanogenic zone. ~~Samples~~As outlined below, samples were analyzed for dissolved Fe(II), CH_4, and $\delta^{13}C_{DIC}$ ~~as outlined below.~~. Additional subsamples for metagenome ~~analysis~~ and lipid ~~analysis~~analyses were taken at the beginning of the experiment and on ~~day~~days 151~~,~~ and ~~day~~ 382, respectively. ~~The purpose of the semi-bioreactors was to set up an experiment that can monitor the redox state regularly, to have a closer to natural conditions, and to have another indication for the processes involving methane in freshly collected sediments.~~

Formatted: Header

Formatted: Footer

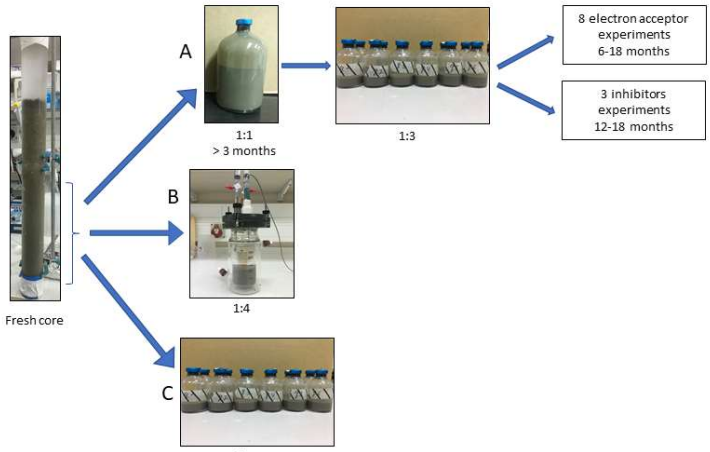

~~Figure 1: Flow diagram of experimental design. Three types of experiments were set up from sediments of the deep methanic zone (below 25 cm): A. Pre-incubated slurry experiments. Fresh sediments collected from the lake were incubated in a 1:1 ratio with porewater extracted from the same depth for 3 months. Then the slurry was divided to the experiments bottles and diluted again with fresh porewater to reach 1:3 ratio. 10 experiments were set up this way, 8 of them with different electron acceptors for 6-18 months, and 3 with different inhibitors for 12-18 months (to one experiment both electron acceptor and an inhibitor were added). B. Semi-bioreactor experiment. Fresh sediments collected from the lake were inserted to two bioreactors and diluted with fresh porewater to reach 1:4 ratio. The bioreactors were set up with no headspace. One of the bioreactors was amended with iron oxide (hematite). C. Slurry experiment with freshly collected sediments. The sediments were diluted with porewater to reach 1:3 ratio, and was amended with different iron oxides (Bar-Or et al., 2017). The experiment was set up for 17 months.~~

2.2.3 ~~Porewater~~Experiment set-up C: Fresh batch experiment

Sediments for this experiment were collected in August 2013 at Station A, similar to the sediments for the pre-incubations. The sediments below 26 cm depth were diluted under anaerobic conditions with porewater from the same depth to reach a 1:5 sediment to porewater ratio. The slurry was divided into 60 ml experiment bottles with 40 ml slurry in each bottle. The sampling and experimental set-up details are described in Bar-Or et al., 2017. Here we present the results of $\delta^{13}C_{DIC}$, metagenome and lipid analyses of two treatments: natural (with only ^{13}C-labeled methane) and hematite. The experiment ran for 15 months.

Formatted: Header

Formatted: Font: Not Bold

Formatted: Justified

Formatted: Font: Not Bold

Formatted: Font: (Default) +Body (Calibri), Not Bold

Formatted: Footer

Formatted: Header

~~About 0.3 ml of filtered (0.22 um) pore-water was injected to~~

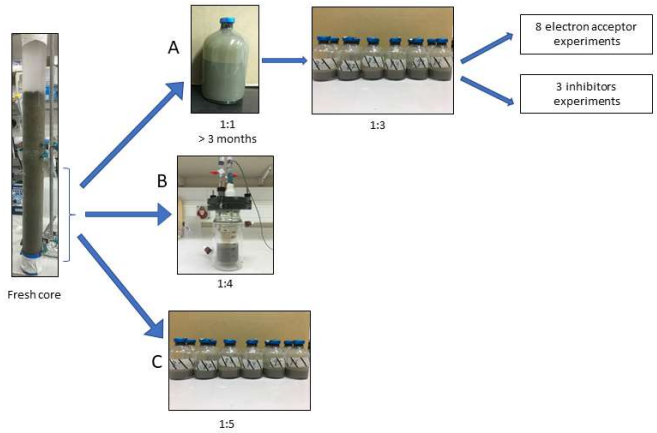

Figure 1: Flow diagram of the experimental design. Three types of experiments were set up from sediments of the methanogenic zone (below 20 cm): A. Two-stage slurry experiments with diluted pre-incubated slurries and porewater (1:3 sediment to porewater ratio). Ten experiments were set up this way, 8 of them with different electron acceptors for 6-18 months, and three different inhibitors for 12-18 months (to one experiment, both electron acceptors and an inhibitor were added). B. Semi-bioreactor experiment with freshly collected sediments. C. Fresh batch experiment -slurry experiment with freshly collected sediments (Bar-Or et al., 2017).

Formatted: Footer

Table 1: Specific details of the three types of experiments: two-stage, semi-bioreactor and fresh batch experiments.

Experiment serial number (SN)	Experiment	Treatment	# of bottles	CH_4 [ml]	$^{13}CH_4$ [ml]	Fe_2O_3 [mM]	Fe_3O_4 [mM]	$Fe(OH)_3$ [mM]	MnO_2 [mM]	NO_3^- [mM]	NO_2^- [mM]	AQDS [mM]	Humic substances [mM]	PCA (mM)	Fe-bearing nontronite (clay) [gr]	Na_2-molybdate [mM]	BES [mM]	Acetylene [µL]	Temp [c°]	Duration [day]	Comments
1	Hematite	$^{12}CH_4$	2		1														20	201	
		13CH4+hematite	2		1	10													20		
2	Magnetite	$^{12}CH_4$	2		1											1			16	447	The methane that was added at the beginning of the experiment was not labelled, so ^{13}C-labeled methane was added after 105 days. Na_2-molybdate was added to one of the bottles on day 365
		$^{12}CH_4$+magnetite	2		1		10												16		Na_2-molybdate was added to one of the bottles on day 365
		$^{12}CH_4$+$Fe(OH)_3$	2		1			10								1			16		
		Killed+$^{12}CH_4$+magnetite	1		1		10												16		
3	MnO_2	$^{12}CH_4$	2		1.2														20	201	200 µL $^{13}CH_4$ was added on day 1, then another 1 mL was added on day 24.
		$^{12}CH_4$+MnO2	2		1.2				10										20		200 µL $^{12}CH_4$ was added on day 1, then another 1 mL was added on day 24.
4	Nitrate	$^{12}CH_4$+NO_3 (high conc.)	2	1	0.5	12				1									20	306	
		$^{12}CH_4$+hematite	2	1	0.5	12													20		
		$^{12}CH_4$+NO_3 (high conc.)+hematite	2	1	0.5	12					1								20		
		$^{12}CH_4$+NO_3 (low conc.)+hematite	2	1	0.5	12					0.2								20		
		Killed+$^{12}CH_4$+NO_3 (high conc.)+hematite	1	1	0.5	12					1								20		
5	Nitrite	$^{12}CH_4$	3	1	0.5														20	493	
		$^{12}CH_4$+NO_2 (high conc.)+hematite	2	1	0.5	10				0.5									20		
		$^{12}CH_4$+NO_2 (low conc.)+hematite	2	1	0.5	10				0.1									20		
		Killed+$^{12}CH_4$+NO_2 (high conc.)+hematite	2	1	0.5	10				0.5									20		
6	AQDS	$^{12}CH_4$	3		1														20	284	
		$^{12}CH_4$+AQDS	2		1							5							20		
		$^{12}CH_4$+AQDS+hematite	2		1	10						5							20		
		Killed+$^{12}CH_4$+AQDS	2		1														20		
7	Natural humic acids and clay	$^{12}CH_4$	2		1														20	169	The head space of the experiment bottles was flushed with N_2 on day 51 and $^{12}CH_4$ was added. This was done in order to match the the clay bottles.
		$^{12}CH_4$+hematite	2		1	10													20		
		$^{12}CH_4$+humic acid	2		1								0.5						20		Clay was added on day 43, and the bottles were flushed again with N_2. $^{12}CH_4$ was added again on day 51.
		$^{12}CH_4$+clay	2		1										1				20		
		Killed+$^{12}CH_4$+hematite	2		1	10													20		
8	Bromoethanesulfonate (BES)	$^{12}CH_4$+hematite	2	9	1	10													20	493	
		$^{12}CH_4$+hematite+BES	2	9	1	10											20		20		
9	Acetylene	$^{12}CH_4$+hematite	4	1	0.5	10												120	20	321	Acetylene was injected to each bottle at different time point during the experiment.
		$^{12}CH_4$+hematite+acetylene	2	1	0.5	10												120	20		
		Killed+$^{12}CH_4$+hematite	2	1	0.5	10													20		
10	No electron acceptor	No additions	3		1														20	147	
		$^{12}CH_4$	3		1														20		
	Semi-bioreactor	$^{12}CH_4$		15															16	345	
		$^{12}CH_4$+hematite		15		10													16	677	
	Freshly collected sediment exp.	$^{12}CH_4$			0.05														20	467	
		$^{12}CH_4$+hematite			0.05	20													20		

Formatted: Header

Formatted: Footer

2.3 Analytical methods

Measurements of $\delta^{13}C_{DIC}$ were performed on a DeltaV Advantage Thermo Scientific isotope-ratio mass-spectrometer (IRMS). Results are reported referent to the Vienna Pee Dee Belemnite (VPDB) standard. For these measurements about 0.3 ml of filtered (0.22 µm) porewater was injected into a 12 ml glass vial with He atmosphere and 10 µl of H_3PO_4 85% to acidify all the DIC species to CO_2 (g). The headspace autosampler takes(CTC Analytics. Type PC PAL) took a gas sample from the vials and measuresmeasured the $\delta^{13}C_{DIC}$ of the sample on the GasBench interface of a DeltaV Advantage Thermo Scientific isotope-ratio mass-spectrometer (IRMS) atwith a precision of ±0.1 ‰. It should be noted that to measure $\delta^{13}C_{CH4}$DIC was measured on the gas sample must be combusted before this procedure, which means thatIRMS using the $\delta^{13}C$ measured is of the DIC only. Results are reported versus the Vienna Pee Dee Belemnite (VPDB) standardpeak height and a precision of 0.05 mM. Dissolved Fe(II) concentrations were measured using the ferrozine method (Stookey, 1970) by a spectrophotometer at 562 nm wavelength with a detection limit of 1 µmol L^{-1}. Methane concentrations were measured from the headspace. A gas100 µL headspace sample was taken from the experiment bottle's headspace bywith a gas-tight syringe and was analyzed for methane and ethylene concentrations by a focus gas chromatograph (GC) equipped with a flame ionization detector (FID) with a detection limit of 50 µmol L^{-1}. Methanogenesis rate was derived from temporal changes in methane concentration in a representative pre-incubated slurry experiment (Fig. S2). The amount of methane oxidized was calculated by a simple mass balance calculation according to Eq. 1 and 2:0.005 µmol. Bottles to which acetylene was added were measured similarly for ethylene to determine the acetylene turnover with the N cycle.

$$x \times F^{13}CH_4 + (1 - x) \times FDI^{13}C_i = FDI^{13}C_f$$

$$[CH_4]_{ox} = x \times [DIC]_f$$

Where x is the mixing fraction of two sources which compose the final DIC; the initial DIC pool and the oxidized ^{13}C-CH_4. The letter x denotes the fraction of oxidized ^{13}C-CH_4, while 1-x denotes the fraction of the initial DIC pool out of the final DIC pool. $F^{13}CH_4$ is the fraction of ^{13}C out of the total CH_4 at t0, $FDI^{13}C_i$ is the fraction of ^{13}C out of the total DIC at t0, and $FDI^{13}C_i$ is the fraction of ^{13}C out of the total DIC at t-final. $[CH_4]_{ox}$ is the amount (concentration in pore water) of the methane oxidized throughout the full incubation period, and $[DIC]_i$ is the DIC concentration at t-final. We assumed that the isotopic composition of the labeled CH_4 did not change significantly throughout the incubation period.

2.4 Lipid analyses

A sub-set of samples (Table 3) was investigated for the assimilation of ^{13}C-labeled methane into polar lipid-derived fatty acids (PLFAs) and intact ether lipid-derived hydrocarbons. A total lipid extract

Formatted: Header

Formatted: Font: Italic

Formatted: Font: Italic

Formatted: Footer

(TLE) was obtained from 0.4 to 1.6 g of the freeze-dried sediment or incubated sediment slurry using a modified Bligh and Dyer protocol (Sturt et al., 2004). Before extraction, 1 µg of 1,2-diheneicosanoyl-*sn*-glycero-3-phosphocholine and 2-methyloctadecanoic acid were added as internal standards. PLFAs in the TLE were converted to fatty acid methyl esters (FAMEs) using saponification with KOH/MeOH and derivatization with BF_3/MeOH (Elvert et al., 2003). Intact archaeal ether lipids in the TLE were separated from the apolar archaeal lipid compounds using preparative liquid chromatography (Meador et al., 2014) followed by ether cleavage with BBr_3 in dichloromethane forming hydrocarbons (Lin et al., 2010). Both FAMEs and ether-cleaved hydrocarbons were analyzed by GC-mass spectrometry (GC-MS; Thermo Finnigan Trace GC coupled to a Trace MS) for identification and GC-IRMS (Thermo Scientific Trace GC coupled via a GC Isolink interface to a Delta V Plus) for ~~the~~ determination of $\delta^{13}C$ values using the column and temperature program settings described by Aepfler et al. (2019)~~.~~. The $\delta^{13}C$ values are reported with an analytical precision better than 1~~–~~‰ as determined by long-term measurements of an *n*-alkane standard with known isotopic composition of each compound. Reported fatty acid isotope data are corrected for the introduction of the methyl group during derivatization by mass balance calculation similar to ~~eq.~~equation 1 using the measured $\delta^{13}C$ value of each FAME and the known isotopic composition of methanol as input parameters.

~~2.5 Metagenome analysis~~

~~Total~~For the metagenomic analyses, total genomic DNA was extracted from the semi-bioreactor experiment (duplicates a and b), pre-incubation ~~1:1 experiments~~slurries ($^{13}CH_4$-only control, $^{13}CH_4$ + hematite) and their respective initial slurries (t0), using the DNeasy PowerLyzer PowerSoil Kit (QIAGEN). ~~Genomic DNA was eluted using 50 µl of elution buffer and stored at −20°C. Metagenomics libraries were prepared at the sequencing core facility at the University of Illinois at Chicago using Nextera XT DNA library preparation kit (Illumina, USA). 19-40 million 2 × 150 bp paired-end reads per library were sequenced using Illumina NextSeq500. For each library, taxonomic diversity was determined by mapping the reads to Silva V138.1 database of the small subunit rRNA sequences using phyloFlash (Glöckner et al., 2017; Gruber-Vodicka et al., 2019).~~Genomic DNA was eluted using 50 µl of elution buffer and stored at −20°C. Metagenomics libraries were prepared at the sequencing core facility at the University of Illinois at Chicago using Nextera XT DNA library preparation kit (Illumina, USA). 19-40 million 2 × 150 bp paired-end reads per library were sequenced using Illumina NextSeq500. Metagenomes were co-assembled from concatenated reads of all metagenomic libraries with Spades V3.12 (Bankevich et al., 2012; Nurk et al., 2013), following decontamination, quality filtering (QV= 10) and adapter-trimming with the BBDuk tool from the BBMap suite (Bushnell B, http://sourceforge.net/projects/bbmap/). Downstream analyses, including ~~read~~reading coverage estimates, automatic binning with maxbin (Wu et al., 2014) and metabat2 (Kang et al., 2019) bin refining with DAS tool (Sieber et al., 2018), were performed within the SqueezeMeta framework (Tamames and Puente-Sánchez, 2019). GTDB-Tk was used to classify the metagenome-assembled

Formatted: Header

Formatted: Font: (Default) +Headings CS (Times New Roman), English (United States)

Formatted: English (United States)

Formatted: Danish

Formatted: Danish

Field Code Changed

Field Code Changed

Formatted: Danish

Formatted: Danish

Field Code Changed

Formatted: Footer

genomes (MAGs) based on Genome Taxonomy Database release 95 (Parks et al., 2021). The principal component analysis biplot was constructed with Past V4.03 (Hammer et al., 2001).

Methanogenesis rate was calculated from temporal changes in methane concentration in a representative pre-incubated slurry experiment (Fig. S3). The amount of methane oxidized was calculated by a simple mass balance calculation according to equations 1 and 2:

$$x \times F^{13}CH_4 + (1-x) \times FDI^{13}C_i = FDI^{13}C_f \quad (1)$$

$$[CH_4]_{ox} = x \times [DIC]_f \quad (2)$$

The final DIC pool comprises two end members; the initial DIC pool and the oxidized ^{13}C-CH_4. The term x denotes the fraction of oxidized ^{13}C-CH_4, while 1-x denotes the fraction of the initial DIC pool out of the final DIC pool. $F^{13}CH_4$ is the fraction of ^{13}C out of the total CH_4 at t0, $FDI^{13}C_i$ is the fraction of ^{13}C out of the total DIC at t0, and $FDI^{13}C_f$ is the fraction of ^{13}C out of the total DIC at t-final. $[CH_4]_{ox}$ is the amount (concentration in pore water) of the methane oxidized throughout the full incubation period, and $[DIC]_f$ is the DIC concentration at t-final. It was assumed that the isotopic composition of the labeled CH_4 did not change significantly throughout the incubation period.

3. Results

In ~~this study~~ten sets of slurry incubation experiments, we followed the progress of the methane oxidation process in (type A) long-term two-stage incubations from Lake Kinneret ~~methanic~~methanogenic sediments~~. This is~~ (Figs. 2 and 3) by ~~quantifying~~monitoring the ~~modifications between experiments conducted on fresh~~ changes $\delta^{13}C_{DIC}$ values, metagenomic and specific isotope lipid analyses. We also followed methane oxidation in a semi-bioreactor system (type B) with freshly collected sediments with or without the addition of hematite (Fig. 2). The results were compared to fresh batch slurry incubations (type C) from the ~~methanic~~same methanogenic zone ~~(batch slurries,~~ presented by Bar-Or et al. (2017) and Elul et al. (2021~~) and semi-bioreactor slurries) and pre-incubated long-term batch slurry experiments.~~).

3.1 Geochemical trends in the two-stage experiments

In the ~~pre-incubated long-term~~two-stage experiments~~, similarly to the fresh incubations,~~ (type A), there was a conversion of ^{13}C-methane to ^{13}C-DIC in all the natural non-killed slurries, indicating significant AOM (Figs. 2- and 3). The $\delta^{13}C_{DIC}$ values ~~in~~of the natural ~~slurries (so called~~ sediment amended only with ^{13}C-methane treatments (the "methane-only" control) reached ~~hundreds of permilles,~~up to 743‰, even with the low abundance of microbial populations in these sediments ~~(Elul et al., 2021)~~. Average AOM rate in the methane-only controls was 2.0±0.4 nmol gr^{-1} dry sediment day^{-1} (Table 2). At the same time, methanogenesis occurred with a net methanogenesis rate of ~ 25 nmol gr dry $sediment^{-1}$ day^{-1}

Formatted: Header
Formatted: Font: Italic
Formatted: Font: Italic
Formatted: No underline
Formatted: Footer

(Fig. S3, Table S2, Table 2.). The two-stage geochemical experiments tested first the potential of several electron acceptors to perform and stimulate the AOM process, as detailed below.

~~The geochemical experiments tested the potential of several~~ 3.1.1 Metals as electron acceptors ~~to perform~~

Iron and ~~stimulate this considerable AOM process. It should be noted that the actual involvement of sulfur cycling can be quantified directly by inhibiting this cycle, while the rest can be tested for their potential involvement by their addition to the slurries. First, metal~~manganese oxides were added~~.~~ as potential electron acceptors. The addition of hematite ~~as an electron acceptor did not change~~to three different treatments increased the $\delta^{13}C_{DIC}$ ~~increase~~values with time ~~(the slope) compared to the methane-only controls (~~and reached up to 694‰ (Fig. 2~~). This is in contrast with the freshly collected sediment experiments, where this addition stimulated the conversion of ^{13}C-methane to ^{13}C-DIC and thus the AOM (Fig. 2). ~~), similarly to the natural (methane-only) controls. The average AOM rate in those treatments was 1.0±0.3 nmol gr dry sediment^{-1} day^{-1} (Table 2). Magnetite amendments resulted in ~~less~~a minor increase ~~in~~of $\delta^{13}C_{DIC}$ values ~~as~~ compared to the methane-only controls (~~to 290~~200‰ and ~~-360~~265‰, respectively, Fig. 3A~~), and amorphous~~) with an AOM rate of 1.8 nmol gr dry sediment^{-1} day^{-1}. Amorphous iron amendments ~~showed even~~ resulted in only a 22‰ increase in $\delta^{13}C_{DIC}$ and a lower ~~values (~~AOM rate (0.1 nmol gr dry sediment^{-1} day^{-1}, Fig. 3A and Table 2). The addition of iron-bearing clay nontronite ~~(iron bearing clay)~~ did not cause any increase in the $\delta^{13}C_{DIC}$ values~~, however, it did result in an increase in the~~ but dissolved Fe(II) concentrations increased compared to the natural methane-only control (Fig. ~~3F~~3B, Fig. ~~S3). The $\delta^{13}C_{DIC}$ values of the bottles with~~4). No AOM was detected 200 days following the addition of MnO_2 ~~also did not show any indication for AOM after 200 days~~based on $\delta^{13}C_{DIC}$ estimates, whereas the $\delta^{13}C_{DIC}$ values of the methane-only controls reached over 500‰ (Fig. ~~3B).~~3F).

~~The actual involvement of sulfate was quantified directly by the addition of Na-molybdate, an inhibitor of sulfate reduction and sulfur disproportionation, to the methane-only controls and to slurries amended with magnetite (Fig. 3A). This addition did not change the slope of the $\delta^{13}C_{DIC}$ increase with time, clearly indicating no AOM inhibition and no role for sulfate in the AOM process. Nitrate was added in two different concentrations (0.2 and 1 mM Fig. 3C) to the long-term~~3.1.2 Sulfate as an electron acceptor

The involvement of sulfate in the AOM of two-stage incubations was tested to detect the feasibility of an active cryptic sulfur cycle, even with the absence of detectable sulfate in the methanogenic sediments (Holmkvist et al., 2011). It was quantified directly by adding Na-molybdate, an inhibitor of sulfate reducers and sulfur disproportionators, to the methane-only controls and slurries amended with

Formatted: Header

Formatted: Footer

magnetite (Fig. 3A). This addition did not change the increase of $\delta^{13}C_{DIC}$ with time, and thus the AOM rates, similar to the observation in the fresh batch incubations (Bar-O et al., 2017).

3.1.3 Nitrate and nitrite as electron acceptors

Nitrate and nitrite involvement in the AOM was tested to detect the feasibility of an active cryptic nitrogen cycle, even with the absence of detectable nitrate and nitrite in the sediments. Nitrate was added at two different concentrations (0.2 and 1 mM, Fig. 3C) to the two-stage slurries amended with hematite, as these concentrations were shown previously to promote AOM in other settings (Ettwig et al., 2010). Hematite addition alone increased the $\delta^{13}C_{DIC}$ values by ~~circa~~ ~200‰ during the 306 days of the experiment. The $\delta^{13}C_{DIC}$ in the bottles with the addition of 1 mM ~~of~~ nitrate, with and without hematite~~,~~ (Fig. 3C; the data points of the two treatments are on top of each other) decreased ~~on the other hand~~ from 43‰ at the beginning of the experiment to 35‰ after 306 days. The $\delta^{13}C_{DIC}$ in the bottles with the addition of 0.2 mM nitrate and hematite increased ~~only slightly in~~by 27‰ at the end of the experiment. We also observed no increase in $\delta^{13}C_{DIC}$ during the first 222 days following the addition of 0.5 mM of nitrite (Fig. 3D), ~~while~~then $\delta^{13}C_{DIC}$ increased by 19‰ ~~afterward~~ until the incubation was terminated. The respective AOM rate was 0.2 nmol gr dry sediment^{-1} day^{-1} (Table 2). Following the addition of 0.1 mM nitrite, $\delta^{13}C_{DIC}$ increased only after 130 days and reached 158‰ at day 493. The respective AOM rate was 0.5 nmol gr dry sediment^{-1} day^{-1}. In the methane-only controls, $\delta^{13}C_{DIC}$ ~~values~~value reached ~~the highest values (~~a maximum of 330~~‰).~~‰.

~~We also~~ 3.1.4 Organic compounds as electron acceptors

Two of the two-stage incubation experiments were amended ~~long-term pre-incubated slurries~~ with ~~potential~~ synthetic and natural organic electron acceptors~~. No $^{13}C_{DIC}$ enrichment was observed with the~~ to test the potential of organic electron acceptors. The addition of AQDS ~~(an analog for humic substrate) to~~ to slurries with and without hematite decreased the $\delta^{13}C_{DIC}$ values during the entire experiment duration (Fig. 3E). ~~Similar trends were observed~~The dissolved Fe(II) showed an increase of 50 µM in ~~$\delta^{13}C_{DIC}$ following the addition of PCA,~~ these treatments, whereas without AQDS there was an ~~analog for methanophenazines that are found in some archaeal membranes and shuttle electrons (Wang and Newman, 2008)~~ increase of 20 µM (Fig. ~~3F~~S4). We further tested the effect of naturally occurring humic substances~~,~~ using those isolated from a different natural lake. The results show that ~~in the beginning~~ the $\delta^{13}C_{DIC}$ values did not change at the beginning of the experiments (Fig. ~~3F~~3B), while a steep increase of ~90 µM in their Fe(II) concentrations ~~was~~were observed (Fig. ~~S3). However, after~~4). After 20 days, the $\delta^{13}C_{DIC}$ values of these slurries started to increase dramatically from 84‰ to 150‰ with ~~a steep slope, indicating high~~an AOM ~~activity~~rate of 1.2 nmol gr dry sediment^{-1} day^{-1} (Fig. ~~3F).~~ ~~We also tested the addition of black coffee, as another example of a complex natural organic substance. In this incubation, again, the $\delta^{13}C_{DIC}$ values decreased during the first 20 days, but then increased very~~

Formatted: Header

Formatted: Default Paragraph Font, Font: (Default) +Headings CS (Times New Roman)

Formatted: Footer

steeply (from 102‰ to 596‰). In those additions there is in general3B, Table 2). We observed a mirrored trend of the dissolved Fe(II) concentrations to that of $\delta^{13}C_{DIC}$ with a steep increase, from 65 to 170 µM, during the first 20 days and thenfollowed by a decrease (from 170of 37 µM to 133 µM, (Fig. S34).

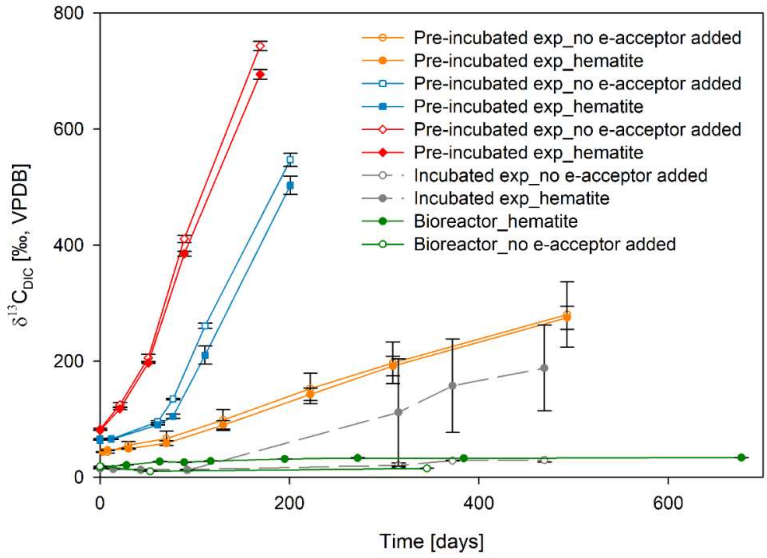

Figure 2: Comparison of $\delta^{13}C_{DIC}$ values between the three types of experiments: three pre-incubated long-term slurry experiments (pre-incubated exp), the bioreactor experiment, and a slurry experiment with freshly collected sediments (incubated exp, (Bar-Or et al., 2017)). In each experiment, two treatments are shown – with hematite (filled symbol) and without (empty symbols) hematite addition. The error bars represent the average deviation of the mean of duplicates/triplicates bottles.

Geochemical analysis of $\delta^{13}C_{DIC}$ was performed also on two experiments that tested the effect of To evaluate which metabolic processes drive AOM, we analyzed $\delta^{13}C_{DIC}$ following the addition of inhibitors on methane metabolism. In one experiment,: i) BES, a specific inhibitor for methanogens and ANME'sANME's *mcrA* genes, was added, and in another experiment,ii) acetylene, a non-specific inhibitor for methanogens, was added. Both cases showed a complete inhibition of labeled ^{13}C-DIC production following the addition, similarly to the killed control (Fig. 45). Acetylene can also inhibit nitrogen cycling in some cases,; however-, this has been shown to result in the production of ethylene is produced then (Oremland and Capone, 1988). In our case, no ethylene was detected, supporting the inhibition only of methanogens'methanogens' activity.

Formatted: Header

Formatted: Footer

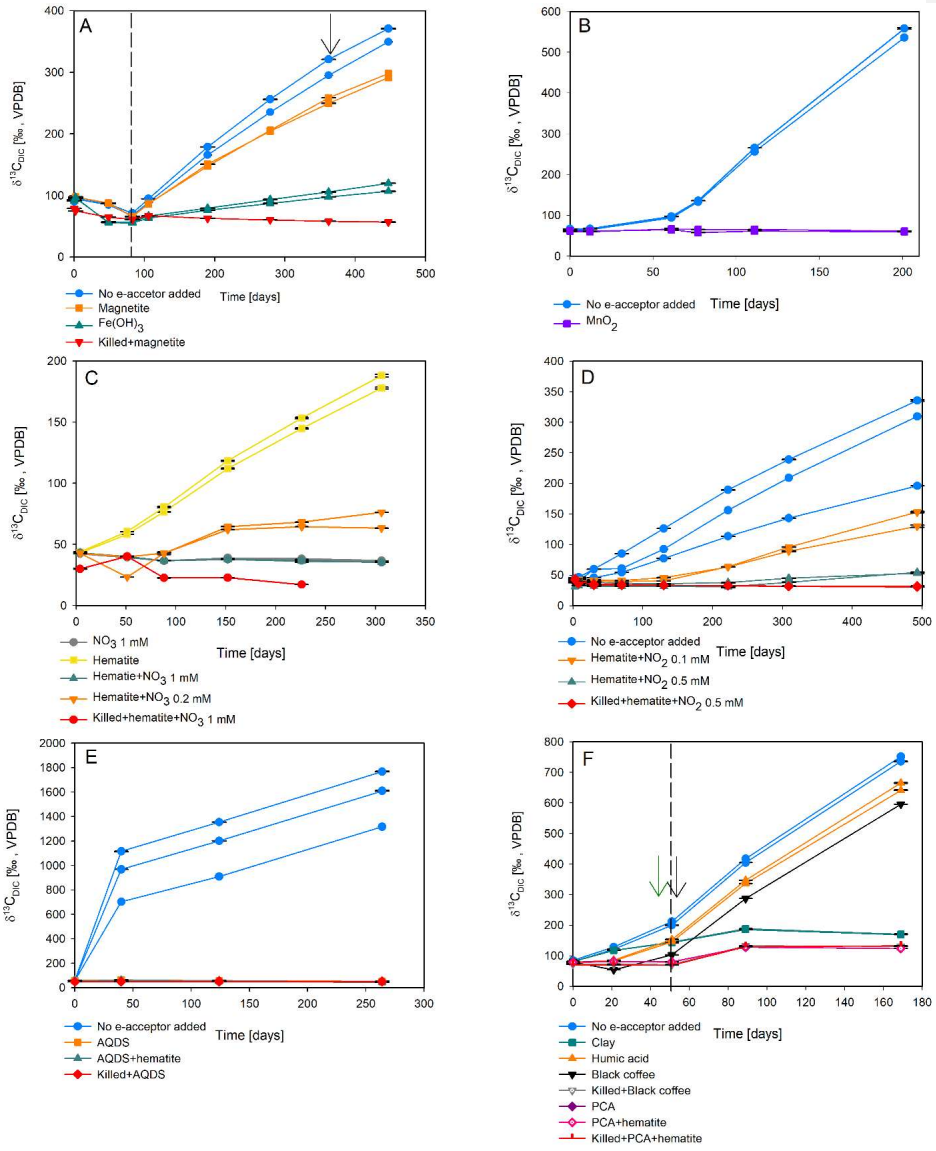

~~Figure 3: The potential of different electron acceptors for AOM in Lake Kinneret sediments. In these pre-incubated long-term slurry experiments, the following treatments have been applied: (A) with and without the addition of magnetite and amorphous iron ($Fe(OH)_3$). Dashed line represents addition of ^{13}C -labeled CH_4. Back arrow represents addition of sodium molybdate as an inhibitor for sulfate reduction. (B) with and without the addition of MnO_2. (C) with the addition of hematite and two different concentrations of nitrate. (D) with the addition of hematite and two different concentrations of nitrite. (E) with the addition of AQDS. (F) with clay, natural humic acid, black coffee and PCA. Green arrow represents the time clay was added to the relevant bottles, the dashed line represents the time the headspace of the bottles was flushed again with N_2, and the black arrow represents the second injection of 1 mL of ^{13}C -labeled methane. ^{13}C -labeled methane was added to all the bottles (specific details on each experiment can be found in Table S2). Each data point is the average of duplicate samples that were taken from each bottle; the error bars are smaller than the symbol.~~

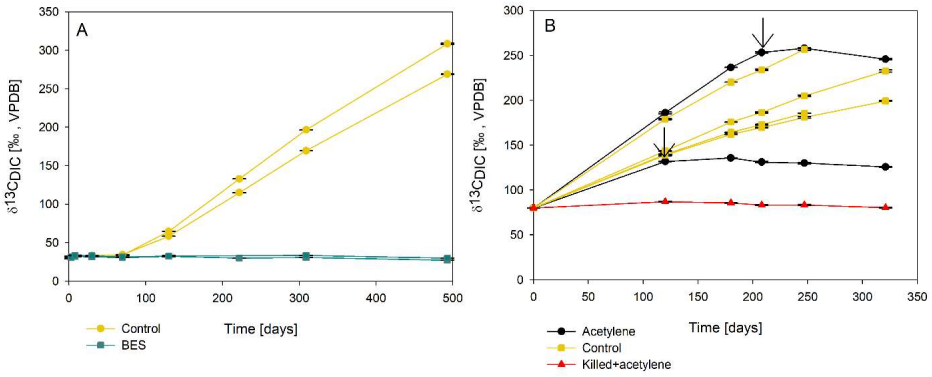

Figure 4: The change of $\delta^{13}C_{DIC}$ values with time in two long-term sediment slurry incubations amended with hematite and ^{13}C-labeled methane. (A) with/out BES and (B) with/out acetylene. Black arrows represent the time point where acetylene was injected to the experiment bottle. The error bars are smaller than the symbols.

3.2 Metagenomic and lipid analyses

The metagenomic analysis points to the potential involvement of several archaea and bacteria in the AOM observed in the pre-incubated slurries. Bona fide ANME (ANME-1), as well as various methanogens and high abundance of Bathyarchaeia were present in all the samples (Table S3). Known sulfate reducing bacteria, including Desulfobacterota, Desulfuromonadota and Thermodesulfovibrionia, but not seep sulfate-reducing bacteria, were found, and some in large read abundances (Table S3). Only very few metagenomic reads mapped to Methylomirabilaceae (NC 10) (<1%) and no reads mapped to *Methanoperedens*. The number of metagenomic reads mapped to functional genes *narH* and *narG*, which encode subunits of the respiratory nitrate reductase in *Methanoperedens* decreased with time in the pre-incubated sediments (Table S4). Very few reads mapped to the *nirS* gene, which encodes the nitrite reductase, and its coverage did not increase over time (Table

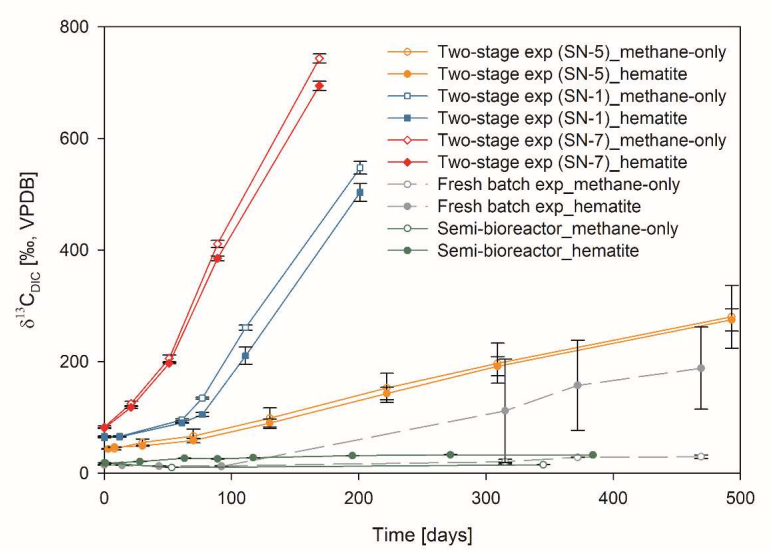

Figure 2: Comparison of $\delta^{13}C_{DIC}$ values among the three types of experiments: A) three two-stage slurry experiments; B) the semi-bioreactor experiment; and C) slurry batch experiment with freshly collected sediments (Bar-Or et al., 2017). In each experiment, two treatments are shown, with hematite (filled symbol) and without (empty symbols) hematite addition. The error bars represent the average deviation of the mean of duplicate/triplicate bottles.

Formatted: Header

Formatted: Footer

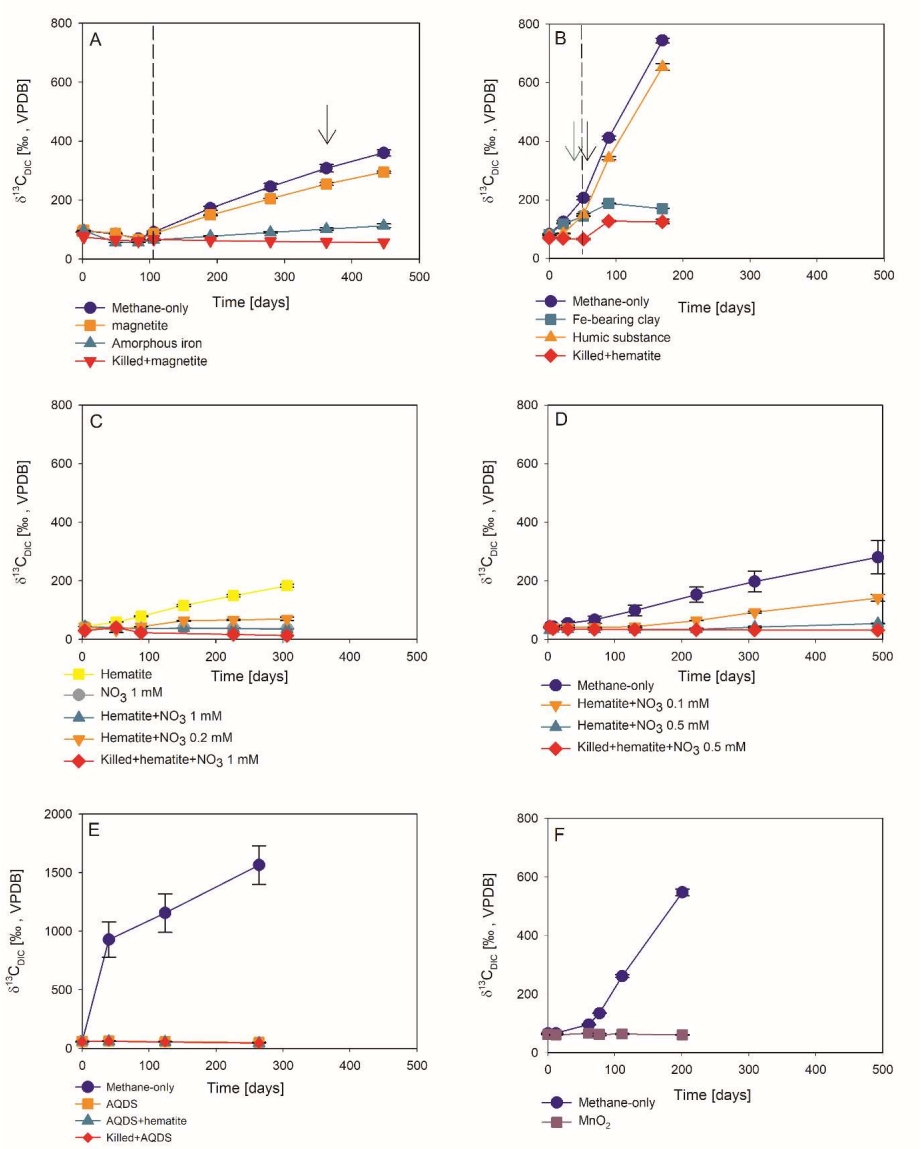

Figure 3: The potential of different electron acceptors for AOM in Lake Kinneret in the pre-incubated long-term slurry experiments with the following treatments: (A) with and without the addition of magnetite and amorphous iron ($Fe(OH)_3$). The dashed line represents the addition of ^{13}C -labeled CH_4. The black arrow represents the addition of Na-molybdate as an inhibitor for sulfate reduction. (B) with clay and natural humic substance. The green arrow represents the time clay was added to the relevant bottles, the dashed line represents the time the headspace of the bottles was flushed again with N_2, and the black arrow represents the second injection of 1 mL of ^{13}C -labeled methane. (C) with the addition of hematite and two different concentrations of nitrate. (D) with the

addition of hematite and two different concentrations of nitrite. (E) with the addition of AQDS. (F) with and without the addition of ^{13}C -labeled methane was added to all the bottles (specific details on each experiment can be found in Table 1). Error bars represent the average of the absolute deviations of data points from their mean.

Table 2: Methanogenesis and AOM rates in experiment A (two-stage slurries) amended with ^{13}C-labeled methane and different electron acceptors (methanogenesis rate was calculated in one of the experiments and was assumed to be similar in all of them).

Experiment serial number (SN)	Treatment	Methanogenesis rate [nmol/gr dry sediment X day]	AOM rate [nmol/gr dry sediment X day]	AOM/methanogenesis [%]
10	**methane only**	24.8	1.1	4.4
1	**methane only**	24.8	1.6	6.4
	methane+hematite	24.8	0.5	2.1
2	**methane only**	24.8	2.4	8.2
	methane+magnetite	24.8	1.8	6.3
	methane+amorphous iron	24.8	0.1	0.5
7	**methane only**	24.8	1.4	6.4
	methane+hematite	24.8	1.3	6.0
	methane+humics	24.8	1.2	5.4
5	**methane only**	24.8	1.0	4.6
	methane+hematite	24.8	1.0	4.6
	methane+hematite+nitrite 0.5 mM	24.8	0.2	0.8
	methane+hematite+nitrite 0.1 mM	24.8	0.5	2.1

Formatted: Header

Formatted: Footer

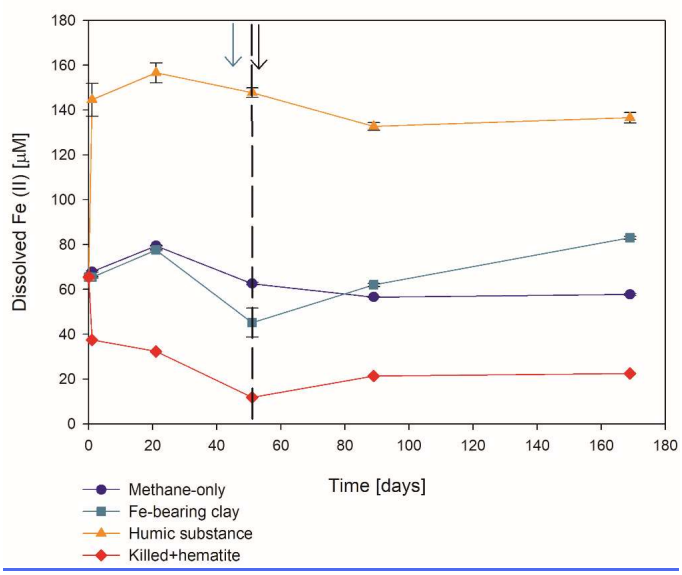

Figure 4: The dissolved Fe(II) change in the two-stage experiment No. 7 containing clay, natural humic acid, and PCA. The green arrow represents the time clay was added to the specific bottles and those bottles flushed with N_2, the dashed line represents the time the rest of the bottles were flushed, and the black arrow represents the time $^{13}CH_4$ was added again. Error bars represent the average of the absolute deviations of data points from their mean.

3.2 Microbial dynamics

Analyses of taxonomy and coverage of metagenome-assembled genomes suggest that in the pre-incubated slurries, Bathyarchaeia are the dominant archaea, together with putative methanogens such as Methanofastidiales (Thermococci), Methanoregulaceae (Methanomicrobia) and Methanotrichales (Methanosarcinia) (Supplementary coverage table). Bonafide ANME (ANME-1) were detected at substantial coverage of approximately 1 (the 27th most abundant out of 195 MAGs) in all the treatments. Among bacteria, sulfate reducers Desulfobacterota and Thermodesulfovibrionales (Nitrospirota) were prominent together with the GIF9 Dehalococcoida lineage, which is known to metabolize chlorinated compounds in lake sediments (Biderre-Petit et al., 2016). Some Methylomirabilales (NC10) were found (average coverage of 0.32±0.06), and no Methanoperedens were detected. Methylococcales methanotrophs were found in the natural sediments and fresh batch and bioreactor incubations (average of 0.34±0.02), as opposed to the average coverage of 0.09±0.04 in long-term incubations. Methylococcales comprised *Methyloterricola*, *Methylomonas* and *Methylobacter* genera (Supplementary coverage table). The methylotrophic partners of aerobic methanotrophs, *Methylotenera*, were found in fresh batch and bioreactor incubations, where *Methylomonas* was found, in line with previous studies showing their association (Beck et al., 2013). Principal component analysis

shows the grouping of long-term pre-incubated slurries, semi-bioreactor incubations, and fresh batch experiments (Fig. 6), emphasizing microbial dynamics over time.

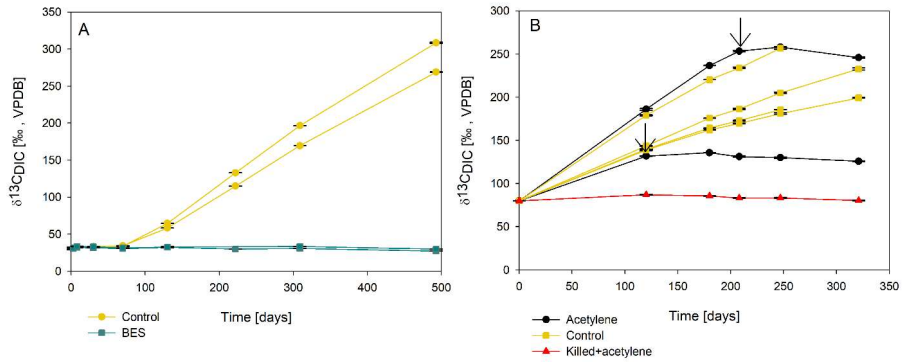

Figure 5: The change of $\delta^{13}C_{DIC}$ values with time in two long-term sediment slurry incubations amended with hematite and ^{13}C-labeled methane. (A) with/out BES and (B) with/out acetylene. Black arrows represent the time at which acetylene was injected to the experiment bottle. The error bars are smaller than the symbols.

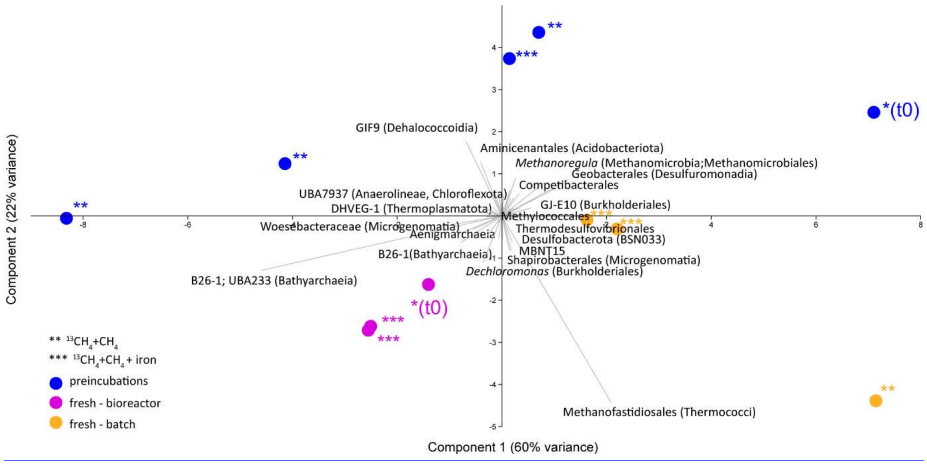

Figure 6: Principal component analysis comparing three types of samples: long-term pre-incubated slurries (blue – experiment A), semi-bioreactor (pink – experiment B) and fresh batch experiments (orange – experiment C). One asterisk represents t0, two asterisks denote methane-only treatments, three asterisks represent hematite treatment.

3.3 Lipid analysis

Formatted: Header

Formatted: Footer

Formatted: Header

~~Table 1: δ^{13}C values (in ‰) of fatty acids and isoprenoid hydrocarbons from different 1:1 incubations and experiments compared to values obtained from the original sediment in the methanic zone.~~

			Fatty acids		Hydrocarbons	
Description	Temperature (°C)	Sampling (days)	$C_{16:1\omega9/8/7}$	$C_{16:1\omega5}$	Phytane	Biphytane
Incubated bottle +$^{13}CH_4$+hematite	20	411	-40	-43	-17	-23
Incubated bottle +$^{13}CH_4$	20	411	-40	-43	-13	-24
Incubated bottle +$^{13}CH_4$	20	1227	-36	-41	-5	-38
[a] Typical fresh sediment incubated bottle hematite+$^{13}CH_4$	20	470	610	1600	-14	-28
Bioreactor+$^{13}CH_4$+hematite	16	382	n.d.	n.d.	n.d.	n.d.
Original sediment (28-30 cm)	14		-44	-50.7	-32	-33

~~S4).~~

~~[a] Bar-Or et al., 2017~~
~~n.d. – Not detected~~

The δ^{13}C values of the archaeol-derived isoprenoid phytane in the long-term pre-incubated samples were between -5 and -17‰ and thus showed a ^{13}C-enrichment ~~(~~between 15-27‰ ~~enrichment), and no ^{13}C-enrichment in the killed control~~relative to the original sediment, indicative of methane-derived carbon assimilation by archaea~~.~~ (Table 3). This ~~signal~~ was ~~also found~~less pronounced for acyclic biphytane ~~but less pronounced (between 5-10‰ enrichment) (Table 1).~~, dominantly derived from caldarchaeol, which showed a ^{13}C-enrichment of 5-10‰. For bacterial-derived fatty acids, the shift in δ^{13}C-values of up to 10‰ relative to the original sediment was in a similar range but would have been expected to be much higher if aerobic methanotrophs were active as was previously indicated by the extreme ^{13}C-enrichment of up to 1,650‰ observed in freshly incubated batch samples (Bar-Or et al., 2017).

Table 3: The δ^{13}C values (in ‰) of fatty acids and isoprenoid hydrocarbons from different experiments compared to values obtained from the original sediment in the methanogenic zone.

Formatted: Footer

~~[a] Bar-Or et al., 2017~~
~~n.d. – Not detected~~

			Fatty acids		Hydrocarbons	
Description	Temperature (°C)	Sampling (days)	$C_{16:1\omega9/8/7}$	$C_{16:1\omega5}$	Phytane	Biphytane
Pre-incubated slurry +$^{13}CH_4$+hematite	20	411	-40	-43	-17	-23
Pre-incubated slurry +$^{13}CH_4$ (bottle A)	20	411	-40	-43	-13	-24
Pre-incubated slurry +$^{13}CH_4$ (bottle B)	20	1227	-36	-41	-5	-38
[a]Fresh batch experiment+$^{13}CH_4$+hematite	20	470	610	1600	-14	-28
Semi-bioreactor+$^{13}CH_4$+hematite	16	382	n.d.	n.d.	n.d.	n.d.
Original sediment (28-30 cm)	14		-44	-51	-32	-33

[a] Bar-Or et al., 2017
n.d. – Not detected

4. Discussion

4.1 AOM is maintained in long-term two-stage incubation experiments

Our ~~many~~previous porewater profiles of Lake Kinneret indicate that microbial sulfate reduction dominates the anoxic hypolimnion and the surface sediments, while methanogenesis is confined to the sediments below the sulfate boundary (Adler et al., 2011; Sivan et al., 2011; Bar-Or et al., 2015~~; Elul et al., 2021). Our previous work on~~). The *in-situ* geochemical and microbial diversity profiles, as well as geochemical and metagenomic analyses of batch incubations with fresh sediments ~~from the lake also~~ , provided evidence for Fe-AOM in the ~~methanie~~deep methanogenic zone ~~based mainly on geochemical and microbiological profiles and models~~below 20 cm depth (Adler et al., 2011; Sivan et al., 2011; Bar-Or et al., 2015~~). It was combined also with measurements of stable carbon isotopes in specific lipids and microbial metagenomic analyses during ^{13}C-labeled methane batch incubations on fresh sediments from the methanic zone (Bar-Or et al., ; Bar-Or et al.,~~ 2017; Elul et al., 2021; Fig. 2). ~~These~~The profiles and the incubations showed ~~the~~an unexpected ~~significant abundance of known~~presence of aerobic bacterial methanotrophs together with anaerobic microorganisms ~~(as methanogens and iron reducers).~~, such as methanogens and iron reducers, in the anoxic sediments. They suggested that both *mcr* gene-bearing archaea and aerobic bacterial methanotrophs mediate methane oxidation. In this study analyses of ^{13}C-DIC derived from ^{13}C-labeled methane suggest that considerable AOM takes place also in the long-term incubations, even after the two stages and the low abundance of the microbial populations. Below, we characterize this AOM process in these incubation experiments.

~~The first noticeable observation from the current pre-incubated long-term slurries data is that the $\delta^{13}C_{DIC}$ values of the natural amendments (only with the addition ^{13}C-labeled methane) increased dramatically. This indicates a clear AOM signal, even after the long-term incubations and the low abundance of the microbial populations. Below, we characterize this AOM process.~~

4.1 Potential electron acceptors for AOM in the long-term ~~pre-incubated~~ two-stage incubation experiments

Formatted: Header

Formatted: No underline

Formatted: Footer

The pre-incubated long-term incubations data show a sharp increase in the $\delta^{13}C_{DIC}$ values of both natural (methane-only) and hematite amendments~~. in the two-stage incubations (Fig. 2).~~ However, ~~as opposed to the freshly collected sediment experiments, there was~~ no difference in $\delta^{13}C_{DIC}$ between the ~~addition of hematite as the electron acceptor and the natural (methane only) amendment. This means that hematite does not have a~~ two treatments was observed following the addition of hematite as the electron acceptor. This differs from the experiments B and C observations with fresh sediment, where the addition of hematite showed higher values than the methane-only treatment (Fig. 2; Bar-Or et al., 2017). This was particularly dramatic in the batch slurries (experiment C), but it was also significant in the semi-bioreactor (experiment B). We believe that the difference in the bioreactors would have been more pronounced if methane concentrations were higher, but it is still significant. The results suggest that either hematite lacks the potential to stimulate the AOM activity during long-term experiments or ~~that there is~~the presence of enough natural Fe(III) in the sediments to sustain the maximum potential of Fe-AOM.

~~Following this observation, we quantified the effect of other metal oxides, such as magnetite, amorphous iron, and manganese oxide (Fig. 3A and B), which are present in Lake Kinneret sediments (Bar-or et al., 2017), on AOM in the long-term incubation slurries from the methanic zone. The results show that the addition of any of these iron oxides showed less increase in the $\delta^{13}C_{DIC}$ values compared to the methane only controls (Figs. 2 and 3). This indicates not only that their addition did not stimulate AOM it might even inhibit it. The less increase in the $\delta^{13}C_{DIC}$ values with their addition could result from their direct inhibition of the AOM process or by their reduction by organic compounds other than methane (organoclastic iron reduction), which added isotopically light carbon from the organics and not heavy carbon from the ^{13}C-labeled methane (masking the natural AOM signal shown in the natural control). We further tested whether ferric iron from clays, which can act as terminal electron acceptors (Kostka et al., 2002; Liu et al., 2011; Liu et al., 2012), could support AOM. However, the addition of the clay minerals appears again to encourage only organoclastic iron reduction (Fig. 3F, Fig. S3). Like iron oxides, manganese oxide, did not support AOM and likely encouraged organoclastic manganese reduction. Given that manganese oxides are found in very low abundance in Lake Kinneret sediments (0.1 %, Table S1), their potential role in metal AOM is likely low anyway.~~

Measurements of $\delta^{13}C_{DIC}$ show that additions of magnetite, amorphous iron, ferric iron from clays and manganese oxide in the two-stage incubations result in a less pronounced increase in the $\delta^{13}C_{DIC}$ values compared to the methane only controls (Figs. 2 and 3), reducing the AOM signal. One possible explanation is that these metal oxides may inhibit AOM, either directly or by a preference for organoclastic iron reduction over Fe-AOM, which adds isotopically light carbon from the organics rather than heavy carbon from the ^{13}C-labeled methane. Using mass-balance estimations in the methane-only treatments and the amorphous iron ones and considering the DIC concentrations and $\delta^{13}C_{DIC}$ values of the methane-only treatments at the beginning of the experiment (6 mM and 60‰, respectively) and

Formatted: Header

Formatted: Footer

the values at the end (6.5 mM and 360‰, respectively), about 0.5 mM of the DIC was added by AOM of methane with $\delta^{13}C$ of ~4000‰. The DIC and $\delta^{13}C_{DIC}$ values of the amorphous iron treatment at the beginning of the experiment were 5.4 mM and 60‰, respectively, and the values at the end were 6.1 mM and 120‰, respectively. Assuming the same $\delta^{13}C$ of the added methane of 4000‰ and $\delta^{13}C_{TOC}$ of -30‰ (Sivan et al., 2011), 0.1 mM of the DIC should derive from AOM and 0.6 mM from organoclastic metabolism. This means that adding amorphous iron to the system decreased the AOM activity and encouraged the oxidation of other organic compounds rather than methane. Intrinsic microbes, particularly the commonly detected ex-deltaproteobacterial lineages such as Geobacterales, may catalyze Fe(III) metal reduction, regardless of AOM. Manganese oxides are found in very low abundance in Lake Kinneret sediments (0.1 %, Table S1). Thus, their role in metal-AOM is likely minimal.

Sulfate concentrations in the ~~methanic~~methanogenic Lake Kinneret sediments are low (< 5 µM, Bar-Or et al., 2015; Elul et al., 2021). Sulfide concentrations ~~are accordingly~~have also been reported to be minor (<0.3 µM, Sivan et al., 2011). However, since pyrite and FeS precipitate in the top sediments, cryptic cycling via pyrite or FeS may replenish sulfate ~~accessible~~available for AOM (Bottrell et al., 2000). ~~The role of sulfate as an electron acceptor was tested directly by the addition of~~ Na-molybdate ~~as an inhibitor for sulfate reduction. This~~ addition to the ~~long-term pre-incubated~~two-stage slurries, including those amended with and without magnetite ~~(Fig. 3A),~~ did not change the $\delta^{13}C_{DIC}$ ~~values, and they increased~~dynamics, which remained similar to those from before the ~~natural (methane only) control, as occurred also~~inhibitor's addition (Fig. 3A). This is in line with the fresh batch sediment slurries (Bar-Or et al., 2017~~). This indicate clearly~~) and hints that sulfate is not ~~involved in the~~ a potent electron acceptor for AOM ~~process in Lake Kinneret methanic sediments, as the inhibition of the sulfur cycling did not inhibit the AOM. This is despite the presence of potential~~in this environment. Furthermore, although sulfate-reducing bacteria ~~as indicated by their relatively high abundance (Table S3) in the sediments.~~ were abundant, none of these reducers belonged to the known clades of ANME partners (Supplementary coverage table).

The ~~concentrations of both,~~ nitrate and nitrite~~,~~ concentrations are ~~also below detection~~undetectable in the porewater of Lake Kinneret sediments (Nüsslein et al., 2001; Sivan et al., 2011), but they may occur as an intermediate product of ammonium oxidation coupled to iron reduction. We thus assessed the role of nitrate and nitrite as electron acceptors in the two-stage slurries. The results indicate that the addition of nitrate delayed AOM and likely promoted denitrification. This is consistent with the fact that ANME-2d was not found. In the case of nitrite, even low concentrations appeared to delay the increase in $\delta^{13}C_{DIC}$ values, suggesting that organoclastic denitrification outcompetes AOM, and nitrite-AOM is not prominent in the two-stage incubations, despite the occurrence of Methylomirabilia (Figs. 3C, D).

Formatted: Header

Formatted: Footer

Humic substances may promote AOM by continuously shuttling electrons to metal oxides (Valenzuela et al., 2019). Humic substances were not measured directly in Lake Kinneret sediments, but the DOC concentrations in porewater at the methanogenic depth were high (~1.5 mM, Adler et al., 2011), suggesting that they play a role in AOM. The addition of the synthetic humic analogs AQDS did not cause any enrichment in ^{13}C-DIC, but an increase of the dissolved Fe(II) concentrations compared to the methane-only treatments. This may be explained by AQDS acting as an electron shuttle in organoclastic iron reduction, producing isotopically light carbon that masks the AOM signal (Fig. 3E, Fig. S4).~~, but their occurrence as an intermediate product through ammonium oxidation coupled to iron reduction (Li et al., 2015; Shuai and Jaffé, 2019) cannot be excluded. Therefore, the potential role of nitrate and nitrite as electron acceptors in the pre-incubated slurries was quantified. The results indicate that rather than stimulating AOM, the addition of nitrate (Fig. 3C) delayed AOM and promoted organoclastic denitrification. Similarly, even low nitrite concentrations appeared to inhibit AOM, potentially facilitating denitrification (Fig. 3D).~~

~~Humic substances were also investigated as potential electron acceptors for the AOM process. They could also promote AOM by continuously shuttling electrons to metal oxides (Valenzuela et al., 2019). Humic substances were not measured specifically in Lake Kinneret sediments, but DOC concentrations in the pore water at the methanic depth were high (~1.5 mM, Adler et al., 2011), suggesting their possible role in the AOM process. The addition of the synthetic humic analogs AQDS did not cause any enrichment in ^{13}C of the DIC. This could be due to their high electron shuttling ability and encouraging organoclastic oxidation that adds light carbon isotope (as opposed to the labeled ^{13}C-methane) and lowers the $\delta^{13}C_{DIC}$ values without AOM at all, or by masking its signal (Fig. 3E). Similar trends were observed in $\delta^{13}C_{DIC}$ following the addition of PCA, a synthetic analog for methanophenazines (Fig. 3F). Yet, the addition of natural humic acids or black coffee exhibited different behavior. At first, the natural humic substances promoted organoclastic iron reduction, probably by shuttling electrons from organic compounds other than methane to natural iron oxides in the sediments (Figs. 3F, S3). Then, perhaps when the availability of the iron oxides or the organic matter decreased, humic substances were used as terminal electron acceptors for AOM, as was suggested by Valenzuela et al. (2017). In that study, AOM was coupled to the reduction of humic substances in the presence of inorganic electron acceptors simultaneously with methanogenesis.~~

~~Overall, our experiments with different electron acceptors indicate clearly that sulfate is not involved in the AOM process in Lake Kinneret methanic sediments, and that~~ Yet, the natural humic substances may support AOM, as was suggested by Valenzuela et al. (2017). In our incubations, the natural humic substances promoted oxidation of organic matter and iron reduction at first, probably by shuttling electrons from organic compounds other than methane to natural iron oxides in the sediments (Figs. 3B and 4). Then, when the availability of the iron oxides or the organic matter decreased, humic substances likely facilitated AOM (Fig. 3B).

Formatted: Header

Formatted: Footer

Overall, our long-term batch experiments, which included different electron acceptors, indicate that sulfate, nitrate, nitrite and Mn-oxides ~~are less likely.~~do not support AOM in Lake Kinneret methanogenic sediments. The potential electron acceptors are natural humic substrates with or without iron minerals that are abundant in the sediment and preferably react with methane rather than with other organics. The involvement of iron oxides in the AOM will be further explored after removing natural iron oxides from the sediments to simulate iron limitation.

4.2 Main microbial players in the long-term pre-incubated ~~experiments~~slurries

~~As mentioned above,~~Methane oxidation in the pre-incubated ~~long-term incubations data show a sharp increase in the $\delta^{13}C_{DIC}$ values of natural amendments. However,~~Lake Kinneret sediments is likely mediated by either ANMEs or methanogens, as the addition of BES, a specific inhibitor for methanogens and ~~ANME's~~ANME's mcrA genes, ~~stopped~~ and acetylene immediately stopped the AOM, similarly to the killed bottles, and ~~to~~ the BES addition to fresh sediment experiments (Bar-Or et a., 2017~~), indicating~~) (Fig. 5). Apart from methane ~~oxidation by methanogens or ANMEs~~ -metabolizing organisms, acetylene can inhibit nitrogen cycling, resulting in ~~all stages of incubations (Fig. 3). In addition, the complete inhibition of labeled DIC~~ethylene production ~~following the addition of acetylene (Fig. 4) suggests the involvement of methane metabolizing microorganisms, also evidenced by the enrichment in~~ (Oremland and Capone, 1988). This is not the case in our incubations, as no ethylene was produced. The increase in $\delta^{13}C$ values ~~of~~in phytane and biphytane (Table ~~1). Such a signal is generally indicative of~~3) also indicates active ~~archaea, i.e.~~archaeal methanogens or ANMEs ~~in this case, which assimilate ^{13}C-carbon from an unknown intermediate or existing DIC.~~(Wegener et al., 2008; Kellermann et al., 2012; Kurth et al., 2019).

~~The essential role of methanogens or ANMEs in the AOM in all stages of incubations suggest that this process is performed by reverse methanogenesis. Indeed, in metagenome-assembled genomes (MAGs) of ANME-1 and *Methanothrix*, all the seven genes (*mcr, mtr, mer, mtd, mch, fir, fmd*) needed for the reverse methanogenesis (Meyerdierks et al., 2010; Wang et al., 2014; Wegener et al., 2021) were found. It should be noted that ANME-1 was found in very low abundance (< 1.5 %) and other ANMEs were not found at all. In addition, while the abundant Bathyarchaeia in all incubation stages might be involved in methane metabolism (Evens et al., 2015), the *mcr-1* genes were not found in their Lake Kinneret MAGs, thus their role in AOM is questionable.~~

~~On the other hand, both the metagenomic and lipid isotopic analysis suggest that the role of aerobic type I methanotrophs (of the class gammaproteobacteria) in methane turnover in the long-term incubations is negligible (Table S3). This contrasts with the natural sediments and fresh incubations that show their presence in the sediments and their important role in oxidizing the methane.~~

Formatted: Header

Formatted: Space Before: 6 pt, After: 12 pt

Formatted: Font: Not Italic

Formatted: Footer

~~**4.3 Methane**~~ Using the isotopic composition of specific lipids and metagenomics, we identified a considerable abundance of aerobic methanotrophs and methylotrophs in the fresh sediments, but not in the pre-incubation slurries (Table 3, Fig. 6), suggesting a minor role of these lineages in the latter. The metagenomic data (Fig. 6, Supplementary coverage table) also indicate that Bathyarchaeia, which might be involved in methane metabolism (Evens et al., 2015), were enriched in the bioreactor incubations, yet their role in Lake Kineret AOM remains to be evaluated. ANME-1 are likely mediators of AOM in these sediments, although methane oxidation via the reverse methanogenesis is feasible for some methanogens in Lake Kinneret sediments (Elul et al., 2021). We also observed changes in abundance of bacterial degraders of organic matter and necromass: for example, GIF9 Dehalococcoidia, which can metabolize complex organics under methanogenic conditions (Cheng et al., 2019; Hug et al., 2013), were most abundant in long-term incubations (Fig. 6, Supplementary coverage table).

4.3 Mechanism of methane oxidation ~~pathway~~ in the long-term incubations – AOM versus back flux

Our results indicate net methanogenesis in ~~long-term incubations~~ the two-stage incubation experiments with an average rate of ~~2 µM~~25 nmol gr^{-1} dry sediment day^{-1} (~~Fig. S2 and~~ Table ~~S5), similarly to the~~2, Fig. S3 and Table S2), similar to fresh incubation experiments (Bar-Or et al., 2017~~). This is even with~~), despite the overall ~~development of~~ increasing trend of $\delta^{13}C_{DIC}$ values resulting from potential methane turnover (~~Fig~~Figs. 2 and 3). A likely explanation for ~~this signal~~both signals is an interplay between methane production and oxidation, with the latter triggered by reverse methanogenesis~~, which is demonstrated among the orders of~~ in bona fide ANMEs or some methanogens ~~and ANMEs~~ (Hallam et al., 2004; Timmers et al., 2017). ~~Of these, *Methanothrix* (closely related to the order Methanosarcinales) has high potential to perform reverse methanogenesis here and in other environmental settings (Valenzuela et al., 2017; 2019; Elul et al., 2021). In our sediments, Methanosarcinales were also found to increase in abundance towards the methanic zone (Bar-Or et al., 2015). Reverse methanogenesis is used in trace methane oxidation by pure cultures of various species of the *Methanosarcina* and the *Methanbacterium* genera (Zehnder and Brock, 1979; Moran et al., 2005, 2007; Luo et al., 2017; Lai et al. 2018).~~

Due to the overall production of methane and the lack of intensive stimulation of AOM by any electron acceptor, the ~~high~~significant increase in $\delta^{13}C_{DIC}$ values could ~~also~~ theoretically result from carbon back flux during methanogenesis, which is feasible in environments close to thermodynamic equilibrium ~~(Gropp et al., 2021). To determine whether back flux is feasible in the incubations, we assessed how much of methane is oxidized and converted to DIC using mass balance calculations. To reach the observed ^{13}C enrichment in our experiments, 3–8 % of the ^{13}C-methane had to be channeled into DIC through Eq. 1 and 2, which is much higher than the previously reported methanogenesis back flux values~~

Formatted: Header

Formatted: Footer

~~(0.3-0.001 %, Zehnder and Brock, 1979; Moran et al., 2005). Back flux reactions have been studied before only in ANME enrichment cultures and by modeling approaches in marine environments without indications~~(Gropp et al., 2021). We used DIC mass balance calculations to determine whether back flux can be accounted for in the incubations. Based on equations 1 and 2, 3-8% of the ^{13}C-methane should be converted into DIC to reach the observed ^{13}C-enrichment. These estimates are orders of magnitude higher than the previously reported 0.001-0.3% values for methanogenesis back flux in cultures (Zehnder and Brock, 1979; Moran et al., 2005), and in the same range of 3.2 to 5.5% of back flux observed in ANME-enrichment cultures (Holler et al., 2011). In contrast, modeling approaches from AOM-dominated marine sediment samples and associated ANME enrichment cultures indicated the absence of net methanogenesis ~~(Holler et al., 2011; (~~Yoshinaga et al., 2014; Chuang et al., 2019; Meister et al., 2019; ~~Wegener et al., 2021). During net AOM conditions, however, this process was recently attributed to intracellular reversibility of enzymes involved in the reaction chain under substrate limitation without invoking methane-DIC equilibration (Wegener et al., 2021). Indeed, low methanogenesis rates in the environment may result in enhanced back flux, compared to the active methanogenic cultures (Hoehler et al., 1994; Holler et al., 2011). Yet, based on the above, it is unlikely that back flux alone will account for the methane-DIC conversion in the Lake Kinneret sediments. Also, we observed no or very little ^{13}C-enrichment in the DIC pool following similar incubations with marine sediments, which showed net methanogenesis and contained similar abundance of methane-metabolizing archaea to that of Lake Kinneret sediments based on the detection of *mcr*A with qPCR~~Wegener et al., 2021). Thus, it is unlikely that back flux alone can account for the methane-DIC conversion in Lake Kinneret sediments. Moreover, just back flux in marine methanogenic sediment with similar net methanogenesis rates and abundant methane-metabolizing archaea did not yield any significant ^{13}C-enrichment in the DIC pool following sediment incubations (Sela-Adler et al., 2015; Amiel, 2018; Vigderovich et al., 2019; Yorshensky, 2019) (Table ~~S6~~S3). Therefore, ~~under natural conditions, methanogens~~methanogenesis back flux alone ~~are unlikely~~seems less likely to ~~produce our~~sustain the observed ~~considerable amounts of~~ DIC ~~just by back flux.~~values than active AOM.

~~4.4 The progression of methane oxidation over time~~

Conclusions

The geochemical and microbial profiles ~~and~~together with fresh sediment incubations ~~show~~showed evidence for Fe-AOM in the ~~methanic~~methanogenic zone of Lake Kinneret, which removes about 10-15% of the produced methane (Adler et al., 2011; Sivan et al., 2011). Anaerobic archaea appear to carry out methane turnover in these reduced sediments by reverse methanogenesis, but ~~methanotrophic~~ aerobic Methylococcales ~~are also~~may be involved in methane oxidation~~. This fits other studies~~, which ~~show more~~ is in line with other evidence ~~pointing to the existence~~ of aerobic bacterial activity in the deep anoxic hypolimnion of lakes and ~~in the~~their shallow sediments (Beck et al., 2013; Oswald et al.,

Formatted: Header

Formatted: Footer

2016; Martinez-Cruz et al., 2017; Cabrol et al., 2020). ~~These bacteria live alongside strict methanogenic anaerobes and iron reducers, probably in a complex interaction, which increases the iron reduction in a cryptic cycle that should be further explored.~~

The simultaneous presence of aerobes and anaerobes ~~together~~ in nature, even 20 meters below the thermocline and oxycline, ~~means that small~~may result from trace amounts of oxygen ~~could be~~ trapped in nano-niches or even in mineral layers ~~(Wang et al., 2018), even if they are not detected by sensitive sensors. This oxygen portion may not be removed by purging the freshly collected sediments~~(Wang et al., 2018), even if sensitive sensors do not detect them. This oxygen portion may not be removed by purging at the beginning of our experiments but is rather slowly used by the methanotrophs for their survival. However, after several incubation stages~~,~~ and intensive purging ~~and~~for a prolonged time, only archaea remained active and were involved in methane turnover~~. It appears that methanotrophic bacteria cannot survive~~, which was most likely coupled to the ~~long-term slurry incubations and thus iron~~ reduction ~~and methane oxidation are decoupled.~~

~~To conclude, trace levels~~ of ~~oxygen may fuel aerobic methane oxidizers in a cryptic cycle between oxygen and iron in the natural lake methanic sediments, and they are responsible for part of the methane oxidation and maybe the iron reduction. The rest of the methane is oxidized to DIC by methanogens or ANME-1. The DIC production from methane turnover in the long-term experiments is performed only by methanogens or ANME-1. It seems less likely that this is by back flux alone, but rather by active metabolic AOM by reverse methanogenesis and an external electron acceptor. Sulfate, nitrate, nitrite, and manganese are unlikely. Humic substances are the most likely~~ electron acceptors ~~used with or without the natural iron oxides~~such as humic substances and iron.

Competing interests. The authors declare that they have no conflict of interest.

Acknowledgements

We would like to thank B. Sulimani and O. Tzabari from the Yigal Allon Kinneret Limnological Laboratory for their onboard technical assistance. We thank all of O. ~~Sivan's~~Sivan's lab members for their help during sampling, and especially to N. Lotem for the help with the mass balance calculations and discussions and to E. Eliani-Russak for her technical assistance. Many thanks to K. Hachmann from M. ~~Elvert's~~Elvert's lab for his help during lipid analysis and to J. Gropp for insightful discussions on the back flux. This work was supported by the ERC consolidator grant (818450) and the Israel Science Foundation (857-2016) of O. Sivan. Funding for M. Elvert was provided by the Deutsche Forschungsgemeinschaft (DFG) (49926684) and EXC 2077 (390741601). Funding for M. Rubin-Blum was provided by the Israel Science Foundation (913/19), the U.S.-Israel Binational Science Foundation (2019055) and Ministry of Science and Technology (1126), and H. Vigderovich was supported by the student fellowship of the Israeli water authority.

Formatted: Header

Formatted: German (Germany)

Formatted: Pattern: Clear (White)

Formatted: Footer

Formatted: Header

References

Adler, Michal, Eckert, W., & Sivan, O. (2011). Quantifying rates of methanogenesis and methanotrophy in Lake Kinneret sediments (Israel) using pore-water profiles. *Limnology and Oceanography*, *56*(4), 1525–1535. https://doi.org/10.4319/lo.2011.56.4.1525

Aepfler, R. F., Bühring, S. I., & Elvert, M. (2019). Substrate characteristic bacterial fatty acid production based on amino acid assimilation and transformation in marine sediments. *FEMS Microbiology Ecology*, *95*(10), 1–15. https://doi.org/10.1093/femsec/fiz131

Amiel, N. (2018). *Authigenic magnetite in deep sediments Authigenic magnetite in deep sediments*.

Aromokeye, D. A., Kulkarni, A. C., Elvert, M., Wegener, G., Henkel, S., Coffinet, S., Eickhorst,T., Oni, O. E., Richter-Heitmann, T., Schnakenberg, A., Taubner, H., Wunder, L., Yin, X., Zhu, Q., Hinrichs, KU., Kasten, S., & Friedrich, M. W. (2020). Rates and Microbial Players of Iron-Driven Anaerobic Oxidation of Methane in Methanic Marine Sediments. *Frontiers in Microbiology*, *10*(January), 1–19. https://doi.org/10.3389/fmicb.2019.03041

Arshad, A., Speth, D. R., De Graaf, R. M., Op den Camp, H. J. M., Jetten, M. S. M., & Welte, C. U. (2015). A metagenomics-based metabolic model of nitrate-dependent anaerobic oxidation of methane by Methanoperedens-like archaea. *Frontiers in Microbiology*, *6*(DEC), 1–14. https://doi.org/10.3389/fmicb.2015.01423

Bai, Y. N., Wang, X. N., Wu, J., Lu, Y. Z., Fu, L., Zhang, F., Lau, TC., & Zeng, R. J. (2019). Humic substances as electron acceptors for anaerobic oxidation of methane driven by ANME-2d. *Water Research*, *164*, 114935. https://doi.org/10.1016/j.watres.2019.114935

Bankevich, A., Nurk, S., Antipov, D., Gurevich, A. a., Dvorkin, M., Kulikov, A. S., Lesin, V. M., Nikolenko, S. I., Pham, S., Prjibelski, A. D., Sirotkin, A. V., Vyahhi, N., Tesler, G., Alekseyev, A. M., & Pevzner, P. a. (2012). SPAdes: A New Genome Assembly Algorithm and Its Applications to Single-Cell Sequencing. *Journal of Computational Biology*, *19*(5), 455–477. https://doi.org/10.1089/cmb.2012.0021

Bar-Or, I., Ben-Dov, E., Kushmaro, A., Eckert, W., & Sivan, O. (2015). *Methane-related changes in prokaryotes along geochemical profiles in sediments of Lake Kinneret (Israel) Methane-related changes in prokaryotes along geochemical profiles in sediments of Lake Kinneret (Israel)*. (August). https://doi.org/10.5194/bg-12-2847-2015

Bar-Or, I., Elvert, M., Eckert, W., Kushmaro, A., Vigderovich, H., Zhu, Q., Ben-Dov, E., & Sivan, O. (2017). Iron-Coupled Anaerobic Oxidation of Methane Performed by a Mixed Bacterial-Archaeal Community Based on Poorly Reactive Minerals. *Environmental Science & Technology*, *51*, 12293–12301. https://doi.org/10.1021/acs.est.7b03126

Beal, E. J., House, C. H., & Orphan, V. J. (2009). Manganese- and Iron-Dependent Marine Methane Oxidation. *Science (New York, N.Y.)*, *325*(5937), 184–187. https://doi.org/10.1126/science.1169984

Formatted: Footer

Beck, D. A. C., Kalyuzhnaya, M. G., Malfatti, S., Tringe, S. G., del Rio, T. G., Ivanova, N., Lidstorm, M. E., & Chistoserdova, L. (2013). A metagenomic insight into freshwater methane-utilizing communities and evidence for cooperation between the Methylococcaceae and the Methylophilaceae. *PeerJ*, *2013*(1), 1–23. https://doi.org/10.7717/peerj.23

Boetius, A., Ravenschlag, K., Schubert, C. J., Rickert, D., Widdel, F., Gieseke, A., Amann, R., Jørgensen, B.B., Witte, U., & Pfannkuche, O. (2000). A marine microbial consortium apparently mediating AOM. *Nature*, *407*(October), 623–626.

Bond, D. R., & Lovley, D. R. (2002). Reduction of Fe(III) oxide by methanogens in the presence and absence of extracellular quinones. *Environmental Microbiology*, *4*(2), 115–124. https://doi.org/10.1046/j.1462-2920.2002.00279.x

Bottrell, S. H., Parkes, R. J., Cragg, B. A., & Raiswell, R. (2000): Isotopic evidence for anoxic pyrite oxidation and stimulation of bacterial sulphate reduction in marine sediments, *J. Geol. Soc. London*,157, 711–714. https://doi.org/10.1144/jgs.157.4.711.

Cabrol, L., Thalasso, F., Gandois, L., Sepulveda-Jauregui, A., Martinez-Cruz, K., Teisserenc, R., Tananaev, N., Tveit, A., Svenning, M. M., & Barret, M. (2020). Anaerobic oxidation of methane and associated microbiome in anoxic water of Northwestern Siberian lakes. *Science of the Total Environment*, *736*, 139588. https://doi.org/10.1016/j.scitotenv.2020.139588

Chuang, P. C., Yang, T. F., Wallmann, K., Matsumoto, R., Hu, C. Y., Chen, H. W., Lin, S., Sun, CH., Li, HC., Wang, Y., & Dale, A. W. (2019). Carbon isotope exchange during anaerobic oxidation of methane (AOM) in sediments of the northeastern South China Sea. *Geochimica et Cosmochimica Acta*, *246*, 138–155. https://doi.org/10.1016/j.gca.2018.11.003

Conrad, R. (2009). The global methane cycle: Recent advances in understanding the microbial processes involved. *Environmental Microbiology Reports*, *1*(5), 285–292. https://doi.org/10.1111/j.1758-2229.2009.00038.x

Dershwitz, P., Bandow, N. L., Yang, J., Semrau, J. D., McEllistrem, M. T., Heinze, R. A., Fonseca, M., Ledesma, J. C., Jennett, J. R., DiSpirito, A. M., Athwal, N. S., Hargrove, M. S., Bobik, T. A., Zischka, H., & DiSpirito, A. A. (2021). Oxygen Generation via Water Splitting by a Novel Biogenic Metal Ion-Binding Compound. *Applied and Environmental Microbiology*, *87*(14), 1–14. https://doi.org/10.1128/aem.00286-21

Eckert, T. (2000). The Influence of Chemical Stratification in the Water Column on Sulfur and Iron Dynamics in Pore Waters and Sediments of Lake Kinneret, Israel. *M.Sc. Thesis*, University of Bayreuth, Germany.

Egger, M., Rasigraf, O., Sapart, C. J., Jilbert, T., Jetten, M. S. M., Röckmann, T., van der Veen, C., Bândă, N., Kartal, B., Ettwig, K. F., & Slomp, C. P. (2015). Iron-mediated anaerobic oxidation of methane in brackish coastal sediments. *Environmental Science and Technology*, *49*(1), 277–283. https://doi.org/10.1021/es503663z

Elul, M., Rubin-Blum, M., Ronen, Z., Bar-Or, I., Eckert, W., & Sivan, O. (2021). Metagenomic insights into the

metabolism of microbial communities that mediate iron and methane cycling in Lake Kinneret sediments. *Biogeosciences Discussions*, 1–24. https://doi.org/10.5194/bg-2020-329

Elvert, M., Boetius, A., Knittel, K., & Jørgensen, B. B. (2003). Characterization of specific membrane fatty acids as chemotaxonomic markers for sulfate-reducing bacteria involved in anaerobic oxidation of methane. *Geomicrobiology Journal*, *20*(4), 403–419. https://doi.org/10.1080/01490450303894

Ettwig, Katharina F, Butler, M. K., Le Paslier, D., Pelletier, E., Mangenot, S., Kuypers, M. M. M., Schreiber, F., Dutilh, B. E., Zedelius, J., de Beer, D. Gloerich, J., Wessels, H. J. C. T., van Alen, T., Luesken, F., Wu, M. L., van de Pas-Schoonen K. T., Op den Camp, H. J. M., Jansen-Megens, E. M., Francoijs, KJ., Stunnenberg, H., Weissenbach, J., Jetten, M. S. M., & Strous, M. (2010). Nitrite-driven anaerobic methane oxidation by oxygenic bacteria. *Nature*, *464*(7288), 543–548. https://doi.org/10.1038/nature08883

Fan, L., Dippold, M. A., Ge, T., Wu, J., Thiel, V., Kuzyakov, Y., & Dorodnikov, M. (2020). Anaerobic oxidation of methane in paddy soil: Role of electron acceptors and fertilization in mitigating CH4 fluxes. *Soil Biology and Biochemistry*, *141*, 107685. https://doi.org/10.1016/j.soilbio.2019.107685

Glöckner, F. O., Yilmaz, P., Quast, C., Gerken, J., Beccati, A., Ciuprina, A., Bruns, G., Yarza, P., Peplies, J., Westram, R., & Ludwig, W. (2017). 25 years of serving the community with ribosomal RNA gene reference databases and tools. *Journal of Biotechnology*, *261*(February), 169–176. https://doi.org/10.1016/j.jbiotec.2017.06.1198

Gropp, J., Iron, M. A., & Halevy, I. (2021). Theoretical estimates of equilibrium carbon and hydrogen isotope effects in microbial methane production and anaerobic oxidation of methane. *Geochimica et Cosmochimica Acta*, *295*, 237–264. https://doi.org/10.1016/j.gca.2020.10.018

Gruber-Vodicka, H. R., Seah, B. K., & Pruesse, E. (2019). phyloFlash — Rapid SSU rRNA profiling and targeted assembly from metagenomes. *BioRxiv*, 521922. https://doi.org/10.1101/521922

Hadas, O., & Pinkas, R. (1995). Sulphate reduction in the hypolimnion and sediments of Lake Kinneret , Israel. *Freshwater Biology*, (33), 63–72.

Hallam, S. J., Putnam, N., Preston, C. M., Detter, J. C., Rokhsar, D., Richardson, P. H., & DeLong, E. F. (2004). Reverse methanogenesis: Testing the hypothesis with environmental genomics. *Science*, *305*(5689), 1457–1462. https://doi.org/10.1126/science.1100025

Haroon, M. F., Hu, S., Shi, Y., Imelfort, M., Keller, J., Hugenholtz, P., Yuan, Z., & Tyson, G. W. (2013). Anaerobic oxidation of methane coupled to nitrate reduction in a novel archaeal lineage. *Nature*, *500*(7464), 567–570. https://doi.org/10.1038/nature12375

He, Q., Yu, L., Li, J., He, D., Cai, X., & Zhou, S. (2019). Electron shuttles enhance anaerobic oxidation of methane coupled to iron(III) reduction. *Science of the Total Environment*, *688*, 664–672. https://doi.org/10.1016/j.scitotenv.2019.06.299

Hoehler, T. M., Alperin, M. J., Albert, D. B., & Martens, C. S. (1994). Field and laboratory, evidence for a

methane-sulfate reducer consortium.pdf. *Global Biogeochemical Cycles*, *8*(4), 451–463.

Holler, T., Wegener, G., Niemann, H., Deusner, C., Ferdelman, T. G., Boetius, A., Brunner, B., & Widdel, F. (2011). Carbon and sulfur back flux during anaerobic microbial oxidation of methane and coupled sulfate reduction. *Proceedings of the National Academy of Sciences of the United States of America*, *108*(52). https://doi.org/10.1073/pnas.1106032108

Holmkvist, L., Ferdelman, T. G., & Jørgensen, B. B. (2011). A cryptic sulfur cycle driven by iron in the methane zone of marine sediment (Aarhus Bay, Denmark). *Geochimica et Cosmochimica Acta*, *75*(12), 3581–3599. https://doi.org/10.1016/j.gca.2011.03.033

Kang, D. D., Li, F., Kirton, E., Thomas, A., Egan, R., An, H., & Wang, Z. (2019). MetaBAT 2: An adaptive binning algorithm for robust and efficient genome reconstruction from metagenome assemblies. *PeerJ*, *2019*(7), 1–13. https://doi.org/10.7717/peerj.7359

Kits, K. D., Klotz, M. G., & Stein, L. Y. (2015). Methane oxidation coupled to nitrate reduction under hypoxia by the Gammaproteobacterium Methylomonas denitrificans, sp. nov. type strain FJG1. *Environmental Microbiology*, *17*(9), 3219–3232. https://doi.org/10.1111/1462-2920.12772

Knittel, K., & Boetius, A. (2009). Anaerobic oxidation of methane: Progress with an unknown process. *Annual Review of Microbiology*, *63*, 311–334. https://doi.org/10.1146/annurev.micro.61.080706.093130

Kostka, J. E., Dalton, D. D., Skelton, H., Dollhopf, S., & Stucki, J. W. (2002). Growth of iron (III)-reducing bacteria on clay minerals as the sole electron acceptor and comparison of growth yields on a variety of oxidized iron forms. *Applied and Environmental Microbiology*, *68*(12), 6256–6262. https://doi.org/10.1128/AEM.68.12.6256-6262.2002

Lai, C. Y., Dong, Q. Y., Rittmann, B. E., & Zhao, H. P. (2018). Bioreduction of Antimonate by Anaerobic Methane Oxidation in a Membrane Biofilm Batch Reactor. *Environmental Science and Technology*, *52*(15), 8693–8700. https://doi.org/10.1021/acs.est.8b02035

Li, X., Hou, L., Liu, M., Zheng, Y., Yin, G., Lin, X., Cheng, L., Li, Y., & Hu, X. (2015). Evidence of Nitrogen Loss from Anaerobic Ammonium Oxidation Coupled with Ferric Iron Reduction in an Intertidal Wetland. *Environmental Science and Technology*, *49*(19), 11560–11568. https://doi.org/10.1021/acs.est.5b03419

Lin, Y. S., Lipp, J. S., Yoshinaga, M. Y., Lin, S. H., Elvert, M., & Hinrichs, K. U. (2010). Intramolecular stable carbon isotopic analysis of archaeal glycosyl tetraether lipids. *Rapid Communications in Mass Spectrometry*, *24*(19), 2817–2826. https://doi.org/10.1002/rcm.4707

Liu, D., Dong, H., Bishop, M. E., Zhang, J., Wang, H., Xie, S., Wang, S., huang, L., & Eberl, D. D. (2012). Microbial reduction of structural iron in interstratified illite-smectite minerals by a sulfate-reducing bacterium. *Geobiology*, *10*(2), 150–162. https://doi.org/10.1111/j.1472-4669.2011.00307.x

Liu, Deng, Dong Hailiang, H., Bishop, M. E., Wang, H., Agrawal, A., Tritschler, S., Eberl, D. D., & Xie, S. (2011). Reduction of structural Fe(III) in nontronite by methanogen Methanosarcina barkeri. *Geochimica et Cosmochimica Acta*, *75*(4), 1057–1071. https://doi.org/10.1016/j.gca.2010.11.009

Lovley, D R, Coates, J. D., BluntHarris, E. L., Phillips, E. J. P., & Woodward, J. C. (1996). Humic substances as electron acceptors for microbial respiration. *Nature*, Vol. 382, pp. 445–448. https://doi.org/10.1038/382445a0

Lovley, Derek R, & Klug, M. J. (1983). Sulfate Reducers Can Outcompete Methanogens at Concentrations Sulfate Reducers Can Outcompete Methanogens Sulfate Concentrationst at Freshwater. *Applied and Environmental Microbiology*, *45*, 187–194.

Luo, J. H., Chen, H., Hu, S., Cai, C., Yuan, Z., & Guo, J. (2018). Microbial Selenate Reduction Driven by a Denitrifying Anaerobic Methane Oxidation Biofilm. *Environmental Science and Technology*, *52*(7), 4006–4012. https://doi.org/10.1021/acs.est.7b05046

Luo, J. H., Wu, M., Yuan, Z., & Guo, J. (2017). Biological Bromate Reduction Driven by Methane in a Membrane Biofilm Reactor. *Environmental Science and Technology Letters*, *4*(12), 562–566. https://doi.org/10.1021/acs.estlett.7b00488

Martinez-cruz, K., Leewis, M., Charold, I., Sepulveda-jauregui, A., Walter, K., Thalasso, F., & Beth, M. (2017). Science of the Total Environment Anaerobic oxidation of methane by aerobic methanotrophs in sub-Arctic lake sediments. *Science of the Total Environment*, *607–608*, 23–31. https://doi.org/10.1016/j.scitotenv.2017.06.187

Meador, T. B., Gagen, E. J., Loscar, M. E., Goldhammer, T., Yoshinaga, M. Y., Wendt, J., Thomm, M., & Hinrichs, K. U. (2014). Thermococcus kodakarensis modulates its polar membrane lipids and elemental composition according to growth stage and phosphate availability. *Frontiers in Microbiology*, *5*(JAN), 1–13. https://doi.org/10.3389/fmicb.2014.00010

Meister, P., Liu, B., Khalili, A., Böttcher, M. E., & Jørgensen, B. B. (2019). Factors controlling the carbon isotope composition of dissolved inorganic carbon and methane in marine porewater: An evaluation by reaction-transport modelling. *Journal of Marine Systems*, *200*(August), 103227. https://doi.org/10.1016/j.jmarsys.2019.103227

Meyerdierks, A., Kube, M., Kostadinov, I., Teeling, H., Glöckner, F. O., Reinhardt, R., & Amann, R. (2010). Metagenome and mRNA expression analyses of anaerobic methanotrophic archaea of the ANME-1 group. *Environmental Microbiology*, *12*(2), 422–439. https://doi.org/10.1111/j.1462-2920.2009.02083.x

Moran, J. J., House, C. H., Freeman, K. H., & Ferry, J. G. (2005). Trace methane oxidation studied in several Euryarchaeota under diverse conditions. *Archaea*, *1*(5), 303–309. https://doi.org/10.1155/2005/650670

Moran, J. J., House, C. H., Thomas, B., & Freeman, K. H. (2007). Products of trace methane oxidation during nonmethyltrophic growth by Methanosarcina. *Journal of Geophysical Research: Biogeosciences*, *112*(2), 1–7. https://doi.org/10.1029/2006JG000268

Newman, D. K., & Kolter, R. (2000). A role for excreted quinones in extracellular electron transfer. *Nature*, *405*(6782), 94–97.

Nollet, L., Demeyer, D., & Verstraete, W. (1997). Effect of 2-bromoethanesulfonic acid and Peptostreptococcus

productus ATCC 35244 addition on stimulation of reductive acetogenesis in the ruminal ecosystem by selective inhibition of methanogenesis. *Applied and Environmental Microbiology*, *63*(1), 194–200. https://doi.org/10.1128/aem.63.1.194-200.1997

Nurk, S., Bankevich, A., & Antipov, D. (2013). Assembling genomes and mini-metagenomes from highly chimeric reads. *Research in Computational Molecular Biology*, 158–170. https://doi.org/10.1007/978-3-642-37195-0

Nüsslein, B., Chin, K. J., Eckert, W., & Conrad, R. (2001). Evidence for anaerobic syntrophic acetate oxidation during methane production in the profundal sediment of subtropical Lake Kinneret (Israel). *Environmental Microbiology*, *3*(7), 460–470. https://doi.org/10.1046/j.1462-2920.2001.00215.x

Oremland, R. S., & Capone, D. G. (1988). *Use of "Specific" Inhibitors in Biogeochemistry and Microbial Ecology* (Vol. 10). https://doi.org/10.2307/4514

Orphan, V. J., House, C. H., & Hinrichs, K. U. (2001). Methane-Consuming Archaea Revealed by Directly Coupled Isotopic and Phylogenetic Analysis. *Science*, *293*(July), 484–488. https://doi.org/10.1126/science.1061338

Oswald, K., Milucka, J., Brand, A., Hach, P., Littmann, S., Wehrli, B., Albersten, M., Daims, H., Wagner, M., Kuypers, M. M. M., Schubert, C. J., & Milucka, J. (2016). Aerobic gammaproteobacterial methanotrophs mitigate methane emissions from oxic and anoxic lake waters. *Limnology and Oceanography*, *61*, S101–S118. https://doi.org/10.1002/lno.10312

Raghoebarsing, A. A., Pol, A., Van De Pas-Schoonen, K. T., Smolders, A. J. P., Ettwig, K. F., Rijpstra, W. I. C., Schouten, S., Sinninghe Damsté, J. S., Op den Camp, H. J. M., Jetten, M. S. M., & Strous, M. (2006). A microbial consortium couples anaerobic methane oxidation to denitrification. *Nature*, *440*(7086), 918–921. https://doi.org/10.1038/nature04617

Ratasuk, N., & Nanny, M. A. (2007). Characterization and quantification of reversible redox sites in humic substances. *Environmental Science and Technology*, *41*(22), 7844–7850. https://doi.org/10.1021/es071389u

Reeburgh, W. S. (2007). Oceanic Methane Biogeochemistry. *ChemInform*, *38*(20), 486–513. https://doi.org/10.1002/chin.200720267

Saunois, M., Stavert, A. R., Poulter, B., Bousquet, P., Canadell, J. G., Jackson, R. B., Raymond, P. A., Dlugokencky, E. J., Houweling, S., Patra, P. K., Ciais, P., Arora, V. K., Bastviken, D., Bergamaschi, P., Blake, D. R., Brailsford, G., Bruhwiler, L., Carlson, K. M., Carrol, M., Castaldi, S., Chandra, N., Crevoisier, C., Crill, P. M., Covey, K., Curry, C. L., Etiope, G., Frankenberg, C., Gedney, N., Hegglin, M. I., Höglund-Isaksson, L., Hugelius, G., Ishizawa, M., Ito, A., Janssens-Maenhout, G., Jensen, K. M., Joos, F., Kleinen, T., Krummel, P. B., Langenfelds, R. L., Laruelle, G. G., Liu, L., Machida, T., Maksyutov, S., McDonald, K. C., McNorton, J., Miller, P. A., Melton, J. R., Morino, I., Müller, J., Murguia-Flores, F., Naik, V., Niwa, Y., Noce, S., O'Doherty, S., Parker, R. J., Peng, C., Peng, S., Peters, G. P., Prigent, C., Prinn, R., Ramonet, M., Regnier, P., Riley, W. J., Rosentreter, J. A., Segers, A., Simpson, I. J., Shi, H.,

Formatted: Header

Formatted: Footer

Smith, S. J., Steele, L. P., Thornton, B. F., Tian, H., Tohjima, Y., Tubiello, F. N., Tsuruta, A., Viovy, N., Voulgarakis, A., Weber, T. S., van Weele, M., van der Werf, G. R., Weiss, R. F., Worthy, D., Wunch, D., Yin, Y., Yoshida, Y., Zhang, W., Zhang, Z., Zhao, Y., Zheng, B., Zhu, Q., Zhu, Q., and Zhuang, Q.: The Global Methane Budget 2000–2017, Earth Syst. Sci. Data, 12, 1561–1623, https://doi.org/10.5194/essd-12-1561-2020, 2020.

Scheller, S., Yu, H., Chadwick, G. L., & Mcglynn, S. E. (2016). *Artificial electron acceptors decouple archaeal methane oxidation from sulfate reduction*. *351*(6274), 1754–1756.

Scheller, S., Yu, H., Chadwick, G. L., McGlynn, S. E., & Orphan, V. J. (2016). Artificial electron acceptors decouple archaeal methane oxidation from sulfate reduction. *Science*, *351*(6274), 1754–1756. https://doi.org/10.1126/science.aad7154

Scott, D. T., Mcknight, D. M., Blunt-Harris, E. L., Kolesar, S. E., & Lovley, D. R. (1998). Quinone moieties act as electron acceptors in the reduction of humic substances by humics-reducing microorganisms. *Environmental Science and Technology*, *32*(19), 2984–2989. https://doi.org/10.1021/es980272q

Segarra, K. E. a, Comerford, C., Slaughter, J., & Joye, S. B. (2013). Impact of electron acceptor availability on the anaerobic oxidation of methane in coastal freshwater and brackish wetland sediments. *Geochimica et Cosmochimica Acta*, *115*, 15–30. https://doi.org/10.1016/j.gca.2013.03.029

Sela-Adler, M., Herut, B., Bar-Or, I., Antler, G., Eliani-Russak, E., Levy, E., Makovsky, Y., & Sivan, O. (2015). Geochemical evidence for biogenic methane production and consumption in the shallow sediments of the SE Mediterranean shelf (Israel). *Continental Shelf Research*, *101*, 117–124. https://doi.org/10.1016/j.csr.2015.04.001

Serruya, C. (1971). Lake Kinneret: the nutrient chemistry of the Sediments. *Limnology and Oceanography*, *16*(May), 510–521.

Shuai, W., & Jaffé, P. R. (2019). Anaerobic ammonium oxidation coupled to iron reduction in constructed wetland mesocosms. *Science of the Total Environment*, *648*, 984–992. https://doi.org/10.1016/j.scitotenv.2018.08.189

Sieber, C. M. K., Probst, A. J., Sharrar, A., Thomas, B. C., Hess, M., Tringe, S. G., & Banfield, J. F. (2018). Recovery of genomes from metagenomes via a dereplication, aggregation and scoring strategy. *Nature Microbiology*, *3*(7), 836–843. https://doi.org/10.1038/s41564-018-0171-1

Sivan, O., Adler, M., Pearson, A., Gelman, F., Bar-Or, I., John, S. G., & Eckert, W. (2011). Geochemical evidence for iron-mediated anaerobic oxidation of methane. *Limnology and Oceanography*, *56*(4), 1536–1544.

Stookey, L. L. (1970). Ferrozine-a new spectrophotometric reagent for iron. *Analytical Chemistry*, *42*(7), 779–781. https://doi.org/10.1021/ac60289a016

Sturt, H. F., Summons, R. E., Smith, K., Elvert, M., & Hinrichs, K. U. (2004). Intact polar membrane lipids in prokaryotes and sediments deciphered by high-performance liquid chromatography/electrospray

Formatted: Header

Formatted: Footer

ionization multistage mass spectrometry - New biomarkers for biogeochemistry and microbial ecology. *Rapid Communications in Mass Spectrometry*, *18*(6), 617–628. https://doi.org/10.1002/rcm.1378

Su, G., Zopfi, J., Yao, H., Steinle, L., Niemann, H., & Lehmann, M. F. (2020). Manganese/iron-supported sulfate-dependent anaerobic oxidation of methane by archaea in lake sediments. *Limnology and Oceanography*, *65*(4), 863–875. https://doi.org/10.1002/lno.11354

Tamames, J., & Puente-Sánchez, F. (2019). SqueezeMeta, A Highly Portable, Fully Automatic Metagenomic Analysis Pipeline. *Frontiers in Microbiology*, *9*. https://doi.org/10.3389/fmicb.2018.03349

Timmers, P. H. A., Welte, C. U., Koehorst, J. J., Plugge, C. M., Jetten, M. S. M., & Stams, A. J. M. (2017). Reverse Methanogenesis and Respiration in Methanotrophic Archaea. *Archaea*, *2017*(Figure 1). https://doi.org/10.1155/2017/1654237

Treude, T., Krause, S., Maltby, J., Dale, A. W., Coffin, R., & Hamdan, L. J. (2014). Sulfate reduction and methane oxidation activity below the sulfate-methane transition zone in Alaskan Beaufort Sea continental margin sediments: Implications for deep sulfur cycling. *Geochimica et Cosmochimica Acta*, *144*, 217–237. https://doi.org/10.1016/j.gca.2014.08.018

Treude, T., Niggemann, J., Kallmeyer, J., Wintersteller, P., Schubert, C. J., Boetius, A., & Jørgensen, B. B. (2005). Anaerobic oxidation of methane and sulfate reduction along the Chilean continental margin. *Geochimica et Cosmochimica Acta*, *69*(11), 2767–2779. https://doi.org/10.1016/j.gca.2005.01.002

Valenzuela, E. I., Avendaño, K. A., Balagurusamy, N., Arriaga, S., Nieto-Delgado, C., Thalasso, F., & Cervantes, F. J. (2019). Electron shuttling mediated by humic substances fuels anaerobic methane oxidation and carbon burial in wetland sediments. *Science of the Total Environment*, *650*, 2674–2684. https://doi.org/10.1016/j.scitotenv.2018.09.388

Valenzuela, E. I., & Cervantes, F. J. (2021). The role of humic substances in mitigating greenhouse gases emissions: Current knowledge and research gaps. *Science of the Total Environment*, *750*, 141677. https://doi.org/10.1016/j.scitotenv.2020.141677

Valenzuela, E. I., Prieto-Davó, A., López-Lozano, N. E., Hernández-Eligio, A., Vega-Alvarado, L., Juárez, K., García-González, A. S., López, M. G., & Cervantes, F. J. (2017). Anaerobic methane oxidation driven by microbial reduction of natural organic matter in a tropical wetland. *Applied and Environmental Microbiology*, *83*(11), 1–15. https://doi.org/10.1128/AEM.00645-17

Vigderovich, H., Liang, L., Herut, B., Wang, F., Wurgaft, E., Rubin-Blum, M., & Sivan, O. (2019). Evidence for microbial iron reduction in the methanogenic sediments of the oligotrophic SE Mediterranean continental shelf. *Biogeosciences Discussions*, 1–25. https://doi.org/10.5194/bg-2019-21

Wang, L., Miao, X., Ali, J., Lyu, T., & Pan, G. (2018). Quantification of Oxygen Nanobubbles in Particulate Matters and Potential Applications in Remediation of Anaerobic Environment. *ACS Omega*, *3*(9), 10624–10630. https://doi.org/10.1021/acsomega.8b00784

Wang, Y., & Newman, D. K. (2008). Redox Reactions of Phenazine Antibiotics with Ferric (Hydr)oxides and

Formatted: Header

Formatted: Footer

Molecular Oxygen. *Environmental Science & Technology*, *42*(7), 2380–2386.

Wang, Z., Guo, F., Liu, L., & Zhang, T. (2014). Evidence of Carbon Fixation Pathway in a Bacterium from Candidate Phylum SBR1093 Revealed with Genomic Analysis. *PLoS ONE*, *9*(10). https://doi.org/10.1371/journal.pone.0109571

Wegener, G., Gropp, J., Taubner, H., Halevy, I., & Elvert, M. (2021). Sulfate-dependent reversibility of intracellular reactions explains the opposing isotope effects in the anaerobic oxidation of methane. *Science Advances*, *7*(19), 1–14. https://doi.org/10.1126/sciadv.abe4939

Wu, Y.-W., Tang, Y.-H., Tringe, S. G., Simmons, B. A., & Singer, S. W. (2014). MaxBin: an automated binning method to recover individual genomes from metagenomes using. *Microbiome*, *2*(26), 4904–4909. Retrieved from https://microbiomejournal.biomedcentral.com/articles/10.1186/2049-2618-2-26

Wuebbles, D. J., & Hayhoe, K. (2002). Atmospheric methane and global change. *Earth-Science Reviews*, *57*(3–4), 177–210. https://doi.org/10.1016/S0012-8252(01)00062-9

Yorshensky, O. (2019). *Iron Reduction in Deep Marine Sediments of the Eastern Mediterranean Continental Shelf and the Yarqon Estuary Iron Reduction in Deep Marine Sediments of the Eastern Mediterranean Continental Shelf and the Yarqon Estuary*. Ben Gurion University of the Negev.

Yoshinaga, M. Y., Holler, T., Goldhammer, T., Wegener, G., Pohlman, J. W., Brunner, B., Kuypers, M. M. M., Hinrichs, K. U., & Elvert, M. (2014). Carbon isotope equilibration during sulphate-limited anaerobic oxidation of methane. *Nature Geoscience*, *7*(3), 190–194. https://doi.org/10.1038/ngeo2069

Zehnder, a J., & Brock, T. D. (1979). Methane formation and methane oxidation by methanogenic bacteria. *Journal of Bacteriology*, *137*(1), 420–432.

Zhang, X., Xia, J., Pu, J., Cai, C., Tyson, G. W., Yuan, Z., & Hu, S. (2019). Biochar-Mediated Anaerobic Oxidation of Methane. *Environmental Science and Technology*, *53*(12), 6660–6668. https://doi.org/10.1021/acs.est.9b01345

Zheng, Y., Wang, H., Liu, Y., Zhu, B., Li, J., Yang, Y., Qin, W., Chen, L., Wu, X., Chistoserdova, L., & Zhao, F. (2020). Methane-Dependent Mineral Reduction by Aerobic Methanotrophs under Hypoxia. *Environmental Science and Technology Letters*, *7*(8), 606–612. https://doi.org/10.1021/acs.estlett.0c00436

Adler, Michal, Eckert, W., & Sivan, O. (2011). Quantifying rates of methanogenesis and methanotrophy in Lake Kinneret sediments (Israel) using porewater profiles. *Limnology and Oceanography*, *56*(4), 1525–1535. https://doi.org/10.4319/lo.2011.56.4.1525

Aepfler, R. F., Bühring, S. I., & Elvert, M. (2019). Substrate characteristic bacterial fatty acid production based on amino acid assimilation and transformation in marine sediments. *FEMS Microbiology Ecology*, *95*(10), 1–15. https://doi.org/10.1093/femsec/fiz131

Amiel, N. (2018). *Authigenic magnetite in deep sediments*. MsC thesis, Ben Gurion University of the Negev.

Formatted: Header

Formatted: Footer

Aromokeye, D. A., Kulkarni, A. C., Elvert, M., Wegener, G., Henkel, S., Coffinet, S., Eickhorst,T., Oni, O. E., Richter-Heitmann, T., Schnakenberg, A., Taubner, H., Wunder, L., Yin, X., Zhu, Q., Hinrichs, KU., Kasten, S., & Friedrich, M. W. (2020). Rates and Microbial Players of Iron-Driven Anaerobic Oxidation of Methane in Methanic Marine Sediments. *Frontiers in Microbiology*, *10*(January), 1–19. https://doi.org/10.3389/fmicb.2019.03041

Arshad, A., Speth, D. R., De Graaf, R. M., Op den Camp, H. J. M., Jetten, M. S. M., & Welte, C. U. (2015). A metagenomics-based metabolic model of nitrate-dependent anaerobic oxidation of methane by Methanoperedens-like archaea. *Frontiers in Microbiology*, *6*(DEC), 1–14. https://doi.org/10.3389/fmicb.2015.01423

Bai, Y. N., Wang, X. N., Wu, J., Lu, Y. Z., Fu, L., Zhang, F., Lau, TC., & Zeng, R. J. (2019). Humic substances as electron acceptors for anaerobic oxidation of methane driven by ANME-2d. *Water Research*, *164*, 114935. https://doi.org/10.1016/j.watres.2019.114935

Bankevich, A., Nurk, S., Antipov, D., Gurevich, A. a., Dvorkin, M., Kulikov, A. S., Lesin, V. M., Nicolenko, S. I., Pham, S., Prjibelski, A. D., Sirotkin, A. V., Vyahhi, N., Tesler, G., Aleksyev, A. M., & Pevzner, P. a. (2012). SPAdes: A New Genome Assembly Algorithm and Its Applications to Single-Cell Sequencing. *Journal of Computational Biology*, *19*(5), 455–477. https://doi.org/10.1089/cmb.2012.0021

Bar-Or, I., Ben-Dov, E., Kushmaro, A., Eckert, W., & Sivan, O. (2015). *Methane-related changes in prokaryotes along geochemical profiles in sediments of Lake Kinneret (Israel) Methane-related changes in prokaryotes along geochemical profiles in sediments of Lake Kinneret (Israel)*. (August). https://doi.org/10.5194/bg-12-2847-2015

Bar-Or, I., Elvert, M., Eckert, W., Kushmaro, A., Vigderovich, H., Zhu, Q., Ben-Dov, E., & Sivan, O. (2017). Iron-Coupled Anaerobic Oxidation of Methane Performed by a Mixed Bacterial-Archaeal Community Based on Poorly Reactive Minerals. *Environmental Science & Technology*, *51*, 12293–12301. https://doi.org/10.1021/acs.est.7b03126

Beal, E. J., House, C. H., & Orphan, V. J. (2009). Manganese-and Iron-Dependent Marine Methane Oxidation. *Science (New York, N.Y.)*, *325*(5937), 184–187. https://doi.org/10.1126/science.1169984

Beck, D. A. C., Kalyuzhnaya, M. G., Malfatti, S., Tringe, S. G., del Rio, T. G., Ivanova, N., Lidstorm, M. E., & Chistoserdova, L. (2013). A metagenomic insight into freshwater methane-utilizing communities and evidence for cooperation between the Methylococcaceae and the Methylophilaceae. *PeerJ*, *2013*(1), 1–23. https://doi.org/10.7717/peerj.23

Biderre-Petit, C., Dugat-Bony, E., Mege, M., Parisot, N., Adrian, L., Moné, A., Denonfoux, J., Peyretaillade, E., Debroas. D., Boucher, D., Peyret, P. (2016). Distribution of Dehalococcoidia in the anaerobic deep water of a remote meromictic crater lake and detection of Dehalococcoidia-derived reductive dehalogenase homologous genes. *PLoS ONE*, *11*(1), 1–19. https://doi.org/10.1371/journal.pone.0145558

Boetius, A., Ravenschlag, K., Schubert, C. J., Rickert, D., Widdel, F., Gieseke, A., Amann, R., Jørgensen, B.B., Witte, U., & Pfannkuche, O. (2000). A marine microbial consortium apparently mediating AOM. *Nature*,

Formatted: Header

Formatted: Footer

407(October), 623–626.

Bottrell, S. H., Parkes, R. J., Cragg, B. A., & Raiswell, R. (2000): Isotopic evidence for anoxic pyrite oxidation and stimulation of bacterial sulphate reduction in marine sediments, *J. Geol. Soc. London*,157, 711–714. https://doi.org/10.1144/jgs.157.4.711.

Cabrol, L., Thalasso, F., Gandois, L., Sepulveda-Jauregui, A., Martinez-Cruz, K., Teisserenc, R., Tananaev, N., Tveit, A., Svenning, M. M., & Barret, M. (2020). Anaerobic oxidation of methane and associated microbiome in anoxic water of Northwestern Siberian lakes. *Science of the Total Environment*, *736*, 139588. https://doi.org/10.1016/j.scitotenv.2020.139588

Cheng, L., Shi, S. bao, Yang, L., Zhang, Y., Dolfing, J., Sun, Y. ge, Liu, L., Li, Q., Tu, B., Dai, L., Shi, Q., & Zhang, H. (2019). Preferential degradation of long-chain alkyl substituted hydrocarbons in heavy oil under methanogenic conditions. *Organic Geochemistry*, *138*. https://doi.org/10.1016/j.orggeochem.2019.103927

Chuang, P. C., Yang, T. F., Wallmann, K., Matsumoto, R., Hu, C. Y., Chen, H. W., Lin, S., Sun, CH., Li, HC., Wang, Y., & Dale, A. W. (2019). Carbon isotope exchange during anaerobic oxidation of methane (AOM) in sediments of the northeastern South China Sea. *Geochimica et Cosmochimica Acta*, *246*, 138–155. https://doi.org/10.1016/j.gca.2018.11.003

Conrad, R. (2009). The global methane cycle: Recent advances in understanding the microbial processes involved. *Environmental Microbiology Reports*, *1*(5), 285–292. https://doi.org/10.1111/j.1758-2229.2009.00038.x

Dershwitz, P., Bandow, N. L., Yang, J., Semrau, J. D., McEllistrem, M. T., Heinze, R. A., Fonseca, M., Ledesma, J. C., Jennett, J. R., DiSpirito, A. M., Athwal, N. S., Hargrove, M. S., Bobik, T. A., Zischka, H., & DiSpirito, A. A. (2021). Oxygen Generation via Water Splitting by a Novel Biogenic Metal Ion-Binding Compound. *Applied and Environmental Microbiology*, *87*(14), 1–14. https://doi.org/10.1128/aem.00286-21

Eckert, T. (2000). The Influence of Chemical Stratification in the Water Column on Sulfur and Iron Dynamics in Pore Waters and Sediments of Lake Kinneret, Israel. *M.Sc. Thesis,* University of Bayreuth, Germany.

Egger, M., Rasigraf, O., Sapart, C. J., Jilbert, T., Jetten, M. S. M., Röckmann, T., van der Veen, C., Bândă, N., Kartal, B., Ettwig, K. F., & Slomp, C. P. (2015). Iron-mediated anaerobic oxidation of methane in brackish coastal sediments. *Environmental Science and Technology*, *49*(1), 277–283. https://doi.org/10.1021/es503663z

Elul, M., Rubin-Blum, M., Ronen, Z., Bar-Or, I., Eckert, W., & Sivan, O. (2021). Metagenomic insights into the metabolism of microbial communities that mediate iron and methane cycling in Lake Kinneret sediments. *Biogeosciences Discussions*, 1–24. https://doi.org/10.5194/bg-2020-329

Elvert, M., Boetius, A., Knittel, K., & Jørgensen, B. B. (2003). Characterization of specific membrane fatty acids as chemotaxonomic markers for sulfate-reducing bacteria involved in anaerobic oxidation of methane. *Geomicrobiology Journal*, *20*(4), 403–419. https://doi.org/10.1080/01490450303894

Ettwig, Katharina F, Butler, M. K., Le Paslier, D., Pelletier, E., Mangenot, S., Kuypers, M. M. M., Schreiber, F., Dutilh, B. E., Zedelius, J., de Beer, D. Gloerich, J., Wessels, H. J. C. T., van Alen, T., Luesken, F., Wu, M. L., van de Pas-Schoonen K. T., Op den Camp, H. J. M., Jansen-Megens, E. M., Francojs, KJ., Stunnenberg, H., Weissenbach, J., Jetten, M. S. M., & Strous, M. (2010). Nitrite-driven anaerobic methane oxidation by oxygenic bacteria. *Nature*, *464*(7288), 543–548. https://doi.org/10.1038/nature08883

Evans, P. N., Parks, D. H., Chadwick, G. L., Robbins, S, J., Orphan V. J., Golding, S. D., & Tyson, G. W. (2015). *Science*. 350(6259), 434-438. http://doi.org/ 10.1126/science.aac7745.

Fan, L., Dippold, M. A., Ge, T., Wu, J., Thiel, V., Kuzyakov, Y., & Dorodnikov, M. (2020). Anaerobic oxidation of methane in paddy soil: Role of electron acceptors and fertilization in mitigating CH4 fluxes. *Soil Biology and Biochemistry*, *141*, 107685. https://doi.org/10.1016/j.soilbio.2019.107685

Gropp, J., Iron, M. A., & Halevy, I. (2021). Theoretical estimates of equilibrium carbon and hydrogen isotope effects in microbial methane production and anaerobic oxidation of methane. *Geochimica et Cosmochimica Acta*, *295*, 237–264. https://doi.org/10.1016/j.gca.2020.10.018

Hadas, O., & Pinkas, R. (1995). Sulphate reduction in the hypolimnion and sediments of Lake Kinneret , Israel. *Freshwater Biology*, (33), 63–72.

Hallam, S. J., Putnam, N., Preston, C. M., Detter, J. C., Rokhsar, D., Richardson, P. H., & DeLong, E. F. (2004). Reverse methanogenesis: Testing the hypothesis with environmental genomics. *Science*, *305*(5689), 1457–1462. https://doi.org/10.1126/science.1100025

Hammer, Ø., Harper, D. A. T., & Ryan, P. D. (2001) Past: paleontological statistics software package for education and data analysis. *Paleontologia-Electronica*. 4 (1), 9.

Haroon, M. F., Hu, S., Shi, Y., Imelfort, M., Keller, J., Hugenholtz, P., Yuan, Z., & Tyson, G. W. (2013). Anaerobic oxidation of methane coupled to nitrate reduction in a novel archaeal lineage. *Nature*, *500*(7464), 567–570. https://doi.org/10.1038/nature12375

Hoehler, T. M., Alperin, M. J., Albert, D. B., & Martens, C. S. (1994). Field and laboratory, evidence for a methane-sulfate reducer consortium.pdf. *Global Biogeochemical Cycles*, *8*(4), 451–463.

Holler, T., Wegener, G., Niemann, H., Deusner, C., Ferdelman, T. G., Boetius, A., Brunner, B., & Widdel, F. (2011). Carbon and sulfur back flux during anaerobic microbial oxidation of methane and coupled sulfate reduction. *Proceedings of the National Academy of Sciences of the United States of America*, *108*(52). https://doi.org/10.1073/pnas.1106032108

Holmkvist, L., Ferdelman, T. G., & Jørgensen, B. B. (2011). A cryptic sulfur cycle driven by iron in the methane zone of marine sediment (Aarhus Bay, Denmark). *Geochimica et Cosmochimica Acta*, *75*(12), 3581–3599. https://doi.org/10.1016/j.gca.2011.03.033

Hug, L. A., Castelle, C. J., Wrighton, K. C., Thomas, B. C., Sharon, I., Frischkorn, K. R., Williams, K. H., Tringe, S. G., & Banfield, J. F. (2013). Community genomic analyses constrain the distribution of metabolic traits across the Chloroflexi phylum and indicate roles in sediment carbon cycling. *Microbiome*,

1(1), 1–17. https://doi.org/10.1186/2049-2618-1-22

Kang, D. D., Li, F., Kirton, E., Thomas, A., Egan, R., An, H., & Wang, Z. (2019). MetaBAT 2: An adaptive binning algorithm for robust and efficient genome reconstruction from metagenome assemblies. *PeerJ*, *2019*(7), 1–13. https://doi.org/10.7717/peerj.7359

Kellermann, M. Y., Wegener, G., Elvert, M., Yoshinaga, M. Y., Lin, Y. S., Holler, T., Mollar, P. X., Knittel K., & Hinrichs, K. U. (2012). Autotrophy as a predominant mode of carbon fixation in anaerobic methane-oxidizing microbial communities. *Proceedings of the National Academy of Sciences of the USA* 109(47), 19321-19326. doi:10.1073/pnas.1208795109.

Kits, K. D., Klotz, M. G., & Stein, L. Y. (2015). Methane oxidation coupled to nitrate reduction under hypoxia by the Gammaproteobacterium Methylomonas denitrificans, sp. nov. type strain FJG1. *Environmental Microbiology*, *17*(9), 3219–3232. https://doi.org/10.1111/1462-2920.12772

Knittel, K., & Boetius, A. (2009). Anaerobic oxidation of methane: Progress with an unknown process. *Annual Review of Microbiology*, *63*, 311–334. https://doi.org/10.1146/annurev.micro.61.080706.093130

Kurth, J.M., Nadine T Smit, Stefanie Berger, Stefan Schouten, Mike S M Jetten, Cornelia U Welte, Anaerobic methanotrophic archaea of the ANME-2d clade feature lipid composition that differs from other ANME archaea, FEMS Microbiology Ecology, Volume 95, Issue 7, July 2019, fiz082.

Li, X., Hou, L., Liu, M., Zheng, Y., Yin, G., Lin, X., Cheng, L., Li, Y., & Hu, X. (2015). Evidence of Nitrogen Loss from Anaerobic Ammonium Oxidation Coupled with Ferric Iron Reduction in an Intertidal Wetland. *Environmental Science and Technology*, *49*(19), 11560–11568. https://doi.org/10.1021/acs.est.5b03419

Lin, Y. S., Lipp, J. S., Yoshinaga, M. Y., Lin, S. H., Elvert, M., & Hinrichs, K. U. (2010). Intramolecular stable carbon isotopic analysis of archaeal glycosyl tetraether lipids. *Rapid Communications in Mass Spectrometry*, *24*(19), 2817–2826. https://doi.org/10.1002/rcm.4707

Lovley, D. R., & Klug, M. J. (1983). Sulfate reducers can outcompete methanogens at freshwater sulfate concentrations. *Applied and Environmental Microbiology*, *45*(1), 187–192. https://doi.org/10.1128/aem.45.1.187-192.1983

Luo, J. H., Chen, H., Hu, S., Cai, C., Yuan, Z., & Guo, J. (2018). Microbial Selenate Reduction Driven by a Denitrifying Anaerobic Methane Oxidation Biofilm. *Environmental Science and Technology*, *52*(7), 4006–4012. https://doi.org/10.1021/acs.est.7b05046

Martinez-cruz, K., Leewis, M., Charold, I., Sepulveda-jauregui, A., Walter, K., Thalasso, F., & Beth, M. (2017). Science of the Total Environment Anaerobic oxidation of methane by aerobic methanotrophs in sub-Arctic lake sediments. *Science of the Total Environment*, *607–608*, 23–31. https://doi.org/10.1016/j.scitotenv.2017.06.187

Meador, T. B., Gagen, E. J., Loscar, M. E., Goldhammer, T., Yoshinaga, M. Y., Wendt, J., Thomm, M., & Hinrichs, K. U. (2014). Thermococcus kodakarensis modulates its polar membrane lipids and elemental composition according to growth stage and phosphate availability. *Frontiers in Microbiology*, *5*(JAN), 1–

13. https://doi.org/10.3389/fmicb.2014.00010

Meister, P., Liu, B., Khalili, A., Böttcher, M. E., & Jørgensen, B. B. (2019). Factors controlling the carbon isotope composition of dissolved inorganic carbon and methane in marine porewater: An evaluation by reaction-transport modelling. *Journal of Marine Systems*, *200*(August), 103227. https://doi.org/10.1016/j.jmarsys.2019.103227

Moran, J. J., House, C. H., Freeman, K. H., & Ferry, J. G. (2005). Trace methane oxidation studied in several Euryarchaeota under diverse conditions. *Archaea*, *1*(5), 303–309. https://doi.org/10.1155/2005/650670

Mosrovaya, A., Wind-Hansen, M., Rousteau, P., Bristow, L. A., & Thamdrup, B. (2021) Sulfate- and iron-dependent anaerobic methane oxidation occuring side-by-side in freshwater lake sediments. *Limnology and Oceanography*. https://doi.org/10.1002/lno.11988

Nollet, L., Demeyer, D., & Verstraete, W. (1997). Effect of 2-bromoethanesulfonic acid and Peptostreptococcus productus ATCC 35244 addition on stimulation of reductive acetogenesis in the ruminal ecosystem by selective inhibition of methanogenesis. *Applied and Environmental Microbiology*, *63*(1), 194–200. https://doi.org/10.1128/aem.63.1.194-200.1997

Nurk, S., Bankevich, A., & Antipov, D. (2013). Assembling genomes and mini-metagenomes from highly chimeric reads. *Research in Computational Molecular Biology*, 158–170. https://doi.org/10.1007/978-3-642-37195-0

Nüsslein, B., Chin, K. J., Eckert, W., & Conrad, R. (2001). Evidence for anaerobic syntrophic acetate oxidation during methane production in the profundal sediment of subtropical Lake Kinneret (Israel). *Environmental Microbiology*, *3*(7), 460–470. https://doi.org/10.1046/j.1462-2920.2001.00215.x

Orembland, R. S., & Capone, D. G. (1988). *Use of "Specific" Inhibitors in Biogeochemistry and Microbial Ecology* (Vol. 10). https://doi.org/10.2307/4514

Orphan, V. J., House, C. H., & Hinrichs, K. (2001). Methane-Consuming Archaea Revealed by Directly Coupled Isotopic and Phylogenetic Analysis. *Science*, *293*(July), 484–488. https://doi.org/10.1126/science.1061338

Oswald, K., Milucka, J., Brand, A., Hach, P., Littmann, S., Wehrli, B., Albersten, M., Daims, H., Wagner, M., Kuypers, M. M. M., Schubert, C. J., & Milucka, J. (2016). Aerobic gammaproteobacterial methanotrophs mitigate methane emissions from oxic and anoxic lake waters. *Limnology and Oceanography*, *61*, S101–S118. https://doi.org/10.1002/lno.10312

Parks, D. H., Chuvochina, M., Rinke, C., Mussig, A. J., Chaumeil, P-A., & Hugenholtz, P. (2021) GTDB: an ongoing census of bacterial and archaeal diversity through a phylogenetically consistent, rank normalized and complete genome-based taxonomy. *Nucleic Acids Research, 202, 1-10.* http://doi.org/10.1093/nar/gkab776

Raghoebarsing, A. A., Pol, A., Van De Pas-Schoonen, K. T., Smolders, A. J. P., Ettwig, K. F., Rijpstra, W. I. C., Schouten, S., Sinninghe Damsté, J. S., Op den Camp, H. J. M., Jetten, M. S. M., & Strous, M. (2006). A

Formatted: Header

Formatted: Footer

microbial consortium couples anaerobic methane oxidation to denitrification. *Nature*, *440*(7086), 918–921. https://doi.org/10.1038/nature04617

Reeburgh, W. S. (2007). Oceanic Methane Biogeochemistry. *ChemInform*, *38*(20), 486–513. https://doi.org/10.1002/chin.200720267

Saunois, M., Stavert, A. R., Poulter, B., Bousquet, P., Canadell, J. G., Jackson, R. B., Raymond, P. A., Dlugokencky, E. J., Houweling, S., Patra, P. K., Ciais, P., Arora, V. K., Bastviken, D., Bergamaschi, P., Blake, D. R., Brailsford, G., Bruhwiler, L., Carlson, K. M., Carrol, M., Castaldi, S., Chandra, N., Crevoisier, C., Crill, P. M., Covey, K., Curry, C. L., Etiope, G., Frankenberg, C., Gedney, N., Hegglin, M. I., Höglund-Isaksson, L., Hugelius, G., Ishizawa, M., Ito, A., Janssens-Maenhout, G., Jensen, K. M., Joos, F., Kleinen, T., Krummel, P. B., Langenfelds, R. L., Laruelle, G. G., Liu, L., Machida, T., Maksyutov, S., McDonald, K. C., McNorton, J., Miller, P. A., Melton, J. R., Morino, I., Müller, J., Murguia-Flores, F., Naik, V., Niwa, Y., Noce, S., O'Doherty, S., Parker, R. J., Peng, C., Peng, S., Peters, G. P., Prigent, C., Prinn, R., Ramonet, M., Regnier, P., Riley, W. J., Rosentreter, J. A., Segers, A., Simpson, I. J., Shi, H., Smith, S. J., Steele, L. P., Thornton, B. F., Tian, H., Tohjima, Y., Tubiello, F. N., Tsuruta, A., Viovy, N., Voulgarakis, A., Weber, T. S., van Weele, M., van der Werf, G. R., Weiss, R. F., Worthy, D., Wunch, D., Yin, Y., Yoshida, Y., Zhang, W., Zhang, Z., Zhao, Y., Zheng, B., Zhu, Q., Zhu, Q., and Zhuang, Q.: The Global Methane Budget 2000–2017, Earth Syst. Sci. Data, 12, 1561–1623, https://doi.org/10.5194/essd-12-1561-2020, 2020.

Scheller, S., Yu, H., Chadwick, G. L., McGlynn, S. E., & Orphan, V. J. (2016). Artificial electron acceptors decouple archaeal methane oxidation from sulfate reduction. *Science*, *351*(6274), 1754–1756. https://doi.org/10.1126/science.aad7154

Segarra, K. E. a, Comerford, C., Slaughter, J., & Joye, S. B. (2013). Impact of electron acceptor availability on the anaerobic oxidation of methane in coastal freshwater and brackish wetland sediments. *Geochimica et Cosmochimica Acta*, *115*, 15–30. https://doi.org/10.1016/j.gca.2013.03.029

Sela-Adler, M., Herut, B., Bar-Or, I., Antler, G., Eliani-Russak, E., Levy, E., Makovsky, Y., & Sivan, O. (2015). Geochemical evidence for biogenic methane production and consumption in the shallow sediments of the SE Mediterranean shelf (Israel). *Continental Shelf Research*, *101*, 117–124. https://doi.org/10.1016/j.csr.2015.04.001

Serruya, C. (1971). Lake Kinneret: the nutrient chemistry of the Sediments. *Limnology and Oceanography*, *16*(May), 510–521.

Shuai, W., & Jaffé, P. R. (2019). Anaerobic ammonium oxidation coupled to iron reduction in constructed wetland mesocosms. *Science of the Total Environment*, *648*, 984–992. https://doi.org/10.1016/j.scitotenv.2018.08.189

Sieber, C. M. K., Probst, A. J., Sharrar, A., Thomas, B. C., Hess, M., Tringe, S. G., & Banfield, J. F. (2018). Recovery of genomes from metagenomes via a dereplication, aggregation and scoring strategy. *Nature Microbiology*, *3*(7), 836–843. https://doi.org/10.1038/s41564-018-0171-1

Sivan, O, Adler, M., Pearson, A., Gelman, F., Bar-Or, I., John, S. G., & Eckert, W. (2011). Geochemical evidence for iron-mediated anaerobic oxidation of methane. *Limnology and Oceanography*, *56*(4), 1536–1544.

Sivan, O., Antler, G., Turchyn, A. V., Marlow, J. J., & Orphan, V. J., (2014). Iron oxides stimulate sulfate-driven anaerobic methane oxidation in seeps. PNAS. 111, E4139-E4147. http://doi.org/10.1073/pnas.1412269111

Sivan, O., Shusta, S., & Valentine, D. L. (2016). Methanogens rapidly transition from methane production to iron reduction. *Geobiology*, 190–203. https://doi.org/10.1111/gbi.12172

Stookey, L. L. (1970). Ferrozine-a new spectrophotometric reagent for iron. *Analytical Chemistry*, *42*(7), 779–781. https://doi.org/10.1021/ac60289a016

Sturt, H. F., Summons, R. E., Smith, K., Elvert, M., & Hinrichs, K. U. (2004). Intact polar membrane lipids in prokaryotes and sediments deciphered by high-performance liquid chromatography/electrospray ionization multistage mass spectrometry - New biomarkers for biogeochemistry and microbial ecology. *Rapid Communications in Mass Spectrometry*, *18*(6), 617–628. https://doi.org/10.1002/rcm.1378

Su, G., Zopfi, J., Yao, H., Steinle, L., Niemann, H., & Lehmann, M. F. (2020). Manganese/iron-supported sulfate-dependent anaerobic oxidation of methane by archaea in lake sediments. *Limnology and Oceanography*, *65*(4), 863–875. https://doi.org/10.1002/lno.11354

Tamames, J., & Puente-Sánchez, F. (2019). SqueezeMeta, A Highly Portable, Fully Automatic Metagenomic Analysis Pipeline. *Frontiers in Microbiology*, *9*. https://doi.org/10.3389/fmicb.2018.03349

Timmers, P. H. A., Welte, C. U., Koehorst, J. J., Plugge, C. M., Jetten, M. S. M., & Stams, A. J. M. (2017). Reverse Methanogenesis and Respiration in Methanotrophic Archaea. *Archaea*, *2017*(Figure 1). https://doi.org/10.1155/2017/1654237

Treude, T., Krause, S., Maltby, J., Dale, A. W., Coffin, R., & Hamdan, L. J. (2014). Sulfate reduction and methane oxidation activity below the sulfate-methane transition zone in Alaskan Beaufort Sea continental margin sediments: Implications for deep sulfur cycling. *Geochimica et Cosmochimica Acta*, *144*, 217–237. https://doi.org/10.1016/j.gca.2014.08.018

Treude, T., Niggemann, J., Kallmeyer, J., Wintersteller, P., Schubert, C. J., Boetius, A., & Jørgensen, B. B. (2005). Anaerobic oxidation of methane and sulfate reduction along the Chilean continental margin. *Geochimica et Cosmochimica Acta*, *69*(11), 2767–2779. https://doi.org/10.1016/j.gca.2005.01.002

Valenzuela, E. I., Avendaño, K. A., Balagurusamy, N., Arriaga, S., Nieto-Delgado, C., Thalasso, F., & Cervantes, F. J. (2019). Electron shuttling mediated by humic substances fuels anaerobic methane oxidation and carbon burial in wetland sediments. *Science of the Total Environment*, *650*, 2674–2684. https://doi.org/10.1016/j.scitotenv.2018.09.388

Valenzuela, E. I., Prieto-Davó, A., López-Lozano, N. E., Hernández-Eligio, A., Vega-Alvarado, L., Juárez, K., García-González, A. S., López, M. G., & Cervantes, F. J. (2017). Anaerobic methane oxidation driven by

microbial reduction of natural organic matter in a tropical wetland. *Applied and Environmental Microbiology*, *83*(11), 1–15. https://doi.org/10.1128/AEM.00645-17

Vigderovich, H., Liang, L., Herut, B., Wang, F., Wurgaft, E., Rubin-Blum, M., & Sivan, O. (2019). Evidence for microbial iron reduction in the methanogenic sediments of the oligotrophic SE Mediterranean continental shelf. *Biogeosciences Discussions*, 1–25. https://doi.org/10.5194/bg-2019-21

Wang, L., Miao, X., Ali, J., Lyu, T., & Pan, G. (2018). Quantification of Oxygen Nanobubbles in Particulate Matters and Potential Applications in Remediation of Anaerobic Environment. *ACS Omega*, *3*(9), 10624–10630. https://doi.org/10.1021/acsomega.8b00784

Wegener G, Niemann H, Elvert M, Hinrichs K-U, Boetius A (2008). Assimilation of methane and inorganic carbon by microbial communities mediating the anaerobic oxidation of methane. Environmental Microbiology 10(9), 2287-2298. doi: 10.1111/j.1462-2920.2008.01653.x.

Wegener, G., Gropp, J., Taubner, H., Halevy, I., & Elvert, M. (2021). Sulfate-dependent reversibility of intracellular reactions explains the opposing isotope effects in the anaerobic oxidation of methane. *Science Advances*, *7*(19), 1–14. https://doi.org/10.1126/sciadv.abe4939

Wu, Y.W., Tang, Y.-H., Tringe, S. G., Simmons, B. A., & Singer, S. W. (2014). MaxBin: an automated binning method to recover individual genomes from metagenomes using. *Microbiome*, *2*(26), 4904–4909. Retrieved from https://microbiomejournal.biomedcentral.com/articles/10.1186/2049-2618-2-26

Wuebbles, D. J., & Hayhoe, K. (2002). Atmospheric methane and global change. *Earth-Science Reviews*, *57*(3–4), 177–210. https://doi.org/10.1016/S0012-8252(01)00062-9

Yorshansky, O. (2019). *Iron Reduction in Deep Marine Sediments of the Eastern Mediterranean Continental Shelf and the Yarqon Estuary*. MsC thesis, Ben Gurion University of the Negev.

Yoshinaga, M. Y., Holler, T., Goldhammer, T., Wegener, G., Pohlman, J. W., Brunner, B., Kuypers, M. M. M., Hinrichs, K. U., & Elvert, M. (2014). Carbon isotope equilibration during sulphate-limited anaerobic oxidation of methane. *Nature Geoscience*, *7*(3), 190–194. https://doi.org/10.1038/ngeo2069

Zehnder, a J., & Brock, T. D. (1979). Methane formation and methane oxidation by methanogenic bacteria. *Journal of Bacteriology*, *137*(1), 420–432.

Zhang, X., Xia, J., Pu, J., Cai, C., Tyson, G. W., Yuan, Z., & Hu, S. (2019). Biochar-Mediated Anaerobic Oxidation of Methane. *Environmental Science and Technology*, *53*(12), 6660–6668. https://doi.org/10.1021/acs.est.9b01345

Zheng, Y., Wang, H., Liu, Y., Zhu, B., Li, J., Yang, Y., Qin, W., Chen, L., Wu, X., Chistoserdova, L., & Zhao, F. (2020). Methane-Dependent Mineral Reduction by Aerobic Methanotrophs under Hypoxia. *Environmental Science and Technology Letters*, *7*(8), 606–612. https://doi.org/10.1021/acs.estlett.0c00436